Diploma Thesis

Morphologic features of alcohol-related liver disease: Correlation with clinical stages and prognostic relevance

submitted by

Patrick Käferböck

attaining the academic degree of

Doctor medicinae universae

(Dr. med. univ.)

at the

Medical University of Graz

conducted at the

Diagnostic- & Research-Institute of Pathology, Medical University of Graz, Austria and

Division of Gastroenterology and Hepatology, Department of Internal Medicine, Medical University of Graz, Austria

under the supervision of

Univ.-Prof. Univ.-Doz. Dr. med. univ. Carolin Lackner

and

Univ.-Prof. Dr. med. univ. Rudolf Stauber

Graz, May 8, 2019

Affidavit (Eidesstattliche Erklärung)

I hereby declare that the following diploma thesis has been written only by the undersigned and without any assistance from third parties. Furthermore, I confirm that no sources have been used in the preparation of this thesis other than those indicated in the thesis itself.

Graz, May 8, 2019 *Patrick Käferböck, eh.*

Acknowledgements

Fist of all, I would like to thank especially Univ.-Prof.in Dr.in Carolin Lackner, who taught me a lot through the conception of my thesis and who inspired me for the topic of histopathology of the liver. She always had an open ear for my numerous questions and concerns and therefore she was not only a mentor but also an important source of support and motivation in that intensive time.

Moreover, I would like to express my gratitude to Univ.-Prof. Dr. Rudolf Stauber, who also was an important, thoughtful and kind supervisor. Thanks also to Dr. Alexander Knisely for his input.

I want to express my great thanks to my parents, Brigitte and Klaus Käferböck, who always believed in me and supported me in all aspects of my life.

What would studying look like, if there was not the important support of friends: Great thank is addressed to all my friends for being there for me during my time in Graz.

Abstract

Introduction

In early stages of alcohol-related liver disease (ALD) centrilobular necroinflammation leads to pericellular collagen deposition around hepatocytes called pericellular fibrosis (PCF). Persisting injury causes septal extension of PCF linking central veins and portal tracts. Progressive fibrosis is characterized by hepatocyte loss from areas of PCF, and development of septal fibrosis (SF) resembling septa in chronic viral hepatitis. We have previously shown that SF and PCF differ with respect to prognosis: histological CRN stage >F2 predicts adverse outcome in compensated ALD while presence of PCF is associated with favorable outcome in decompensated ALD.

This study aimed to investigate the association of SF and PCF, as quantified by digital image analysis on survival in compensated and decompensated ALD.

Patients and Methods

We investigated 166 patients with ALD (compensated, n=50; decompensated, n=116) without other causes of liver disease. Clinical and biochemical factors and date of liver-related death were retrieved from the medical history. Median follow up time was 4.3 years. SF and PCF were manually distinguished using digitized slides and Collagen proportionate areas (CPA) for total fibrosis (TF), SF, PCF and parenchymal proportionate area (PPA) were quantified using Definiens ™ software. The effects of fibrosis types and PPA on 5-year survival were assessed by Kaplan-Meier analysis and log-rank test. Optimized cut offs were determined by Youden index.

Results

In the compensated group, TF ($p=0.009$) and SF ($p=0.008$) but not PCF predicted worse outcome; however, survival was best predicted by the PCF/SF ratio ($p<0.001$). In the decompensated group consisting mostly of cirrhotics, worse outcome tended to associate with SF ($p=0.078$) and TF ($p=0.165$) but was inversely associated with PCF ($p=0.076$). The PCF/SF ratio ($p=0.001$) again was a better predictor of survival than any of the individual fibrosis types. PPA was associated with outcome in compensated but not decompensated ALD (respectively $p=0.017$ and $p=0.135$).

Discussion

In our study we could confirm that quantitatively assessed SF and PCF are associated with different outcomes. PCF/SF ratio is a better predictor of survival than is TF, SF or PCF alone. The prognostic value of assessing fibrosis by type in ALD should be investigated in further studies.

Zusammenfassung

Einleitung

Am Krankheitsbeginn der alkohol-assoziierten Lebererkrankungen (ALD) führen zentrolobuläre nekrotisierende Entzündungsreaktionen zu einer, die Hepatozyten umgebenden, Kollagenablagerung, welche perizelluläre Fibrose (PCF) genannt wird. Bleibt der schädigende Einfluss bestehen kommt es zu einer septalen Ausdehnung der PCF, welche Zentralvenen und Portalfelder verbindet. Fortgeschrittene Fibrose ist schließlich durch einen Verlust von Hepatozyten aus Arealen mit PCF, sowie dem Entstehen der septalen Fibrose (SF), vergleichbar mit Septen der chronischen viralen Hepatitis, gekennzeichnet. In Voruntersuchungen konnten wir zeigen, dass SF und PCF Unterschiede hinsichtlich des Krankheitsverlaufes zeigen. Ein histologischer CRN Stage > F2 in kompensierter ALD ist mit schlechteren, wohingegen PCF in dekompensierter ALD auf einen besseren Krankheitsverlauf hindeutet.

Das Ziel dieser Studie ist einen Zusammenhang von SF und PCF, welche mit digitaler Bildanalyse quantifiziert werden, und dem Überleben von PatientInnen sowohl mit kompensierter als auch mit dekompensierter ALD zu untersuchen.

PatientInnen und Methode

Es wurden 166 PatientInnen mit ALD (kompensiert, n=50; dekompensiert, n=116) ohne andere Ursachen der Lebererkrankung untersucht. Klinische und biochemische Daten, sowie das Datum des leber-assoziierten Todes, wurden aus der Krankengeschichte erhoben. Die PatientInnen wurden im Median 4.3 Jahre nachverfolgt. SF und PCF wurden an digitalen Objektträgern manuell aufgetrennt. Die Collagen Proportionate Area (CPA) für die Geamtfibrose (TF), SF und PCF, sowie die Parenchymfläche (PPA), wurden mittels Definiens TM Software quantifiziert. Der Einfluss der Fibrosetypen und der PPA auf das 5-Jahres-Überleben wurde mittels Kaplan-Meier Analyse und Log-Rang-Test ermittelt. Die optimalen Cut-off-Werte wurden mit Hilfe des Youden-Index berechnet.

Ergebnisse

In der kompensierten Gruppe sagten TF ($p=0.009$) und SF ($p=0.008$), nicht jedoch PCF, einen schlechteren Krankheitsverlauf voraus. Das Überleben hingegen wurde durch das Verhältnis von PCF zu SF am besten prognostiziert ($p<0.001$). In

der dekompensierten Gruppe, welche vorwiegend aus Zirrhosen besteht, zeigte sich eine Tendenz zu schlechterem Krankheitsverlauf bei SF (p=0.078) und TF (p=0.165), bei PCF (p=0.076) jedoch umgekehrt. Das Verhältnis wiederum war ein besserer Prädiktor des Überlebens als alle individuellen Fibrosetypen. Die PPA war in der kompensierten (p=0.017), nicht jedoch in der dekompensierten Gruppe (p=0.135) mit dem Krankheitsverlauf assoziiert.

Diskussion

Wir konnten in unserer Untersuchung zeigen, dass die quantifizierte SF und PCF im Zusammenhang mit dem Krankheitsverlauf stehen. Das Verhältnis von PCF zu SF sagt das Überleben besser voraus, als TF, SF oder PCF alleine. Die prognostische Relevanz der verschiedenen Fibrosetypen sollte in weiteren Studien genauer evaluiert werden.

List of contents

Index of Abbreviations

ADH	Alcohol dehydrogenase
ALD	Alcohol-related liver disease
ALT	Alanine aminotransferase
AH	Alcoholic hepatitis
AP	Alkaline phosphatase
ASH	Steatohepatitis due to alcohol
AST	Aspatate aminotransferase
AUC	Area under the curve
AUD	Alcoholic use disorder
AUDIT	Alcohol use disorder identification test
BMI	Body mass index
CAB	Chromotrope -aniline blue
CPA	Collagen proportionate area
CPS	Child-Pugh-score
CRN	Clinical Research Network
FIB	Fibrosis
GGT	Gamma-glutamyl-transferase
HE	Hepatic encephalopathy
H&E	Haematoxylin and Eosin Stain
INR	International Normalized Ratio
MDB	Mallory-Denk-Bodies
MDF	Maddrey’s discriminant function
MELD	Model for End Stage Liver Disease
MEOS	Microsomal ethanol-oxidizing system

NAD	Nicotinamide adenine dinucleotide
NAFLD	Non-alcoholic fatty liver disease
PAR	Parenchyma
PPA	Parenchymal proportionate area
SD	Standard deviation
SR	Sirius-red stain
TE	Transient elastography
THV	Terminal hepatic vein

Index of Figures

Index of Tables

1 Introduction

1.1 Epidemiology

The global status report on alcohol and health 2014 of the World Health Organization (1) reports that 50 percent of liver cirrhosis cases are attributable to extensive alcohol consumption. The amount of alcohol consumption varies around the globe with the highest intake per person per year in Europe (1).

The EASL Clinical Practice Guidelines of the Management of Alcohol-Related Liver Disease issued a consensus about the definitions of amount of alcohol contained in a standard drink and the types of drinking. To provide a basis for the comparability of data between studies one drink is defined to contain ten grams of pure alcohol and heavy episodic drinking as the consumption of six drinks (60 g alcohol) on one occasion (2).

The community-based assumption, that the intake of low amounts of alcohol is health protective, is not supported among experts, because the negative consequences (like the fact that alcohol is a carcinogen) outweigh the health benefits (2). Bagnardi et. al. (3) found in their meta-analysis including 572 studies a dose-response relationship between alcohol ingestion and a broad variety of cancers, e.g., oral and pharyngeal cancer or esophageal squamous cell carcinoma.

Corrao et. al. (4) reported in a meta-analysis that consuming 25 g alcohol per day significantly increases the risk of developing alcohol-related liver disease (ALD).

There is strong evidence, that abstinence is a cornerstone in the management of ALD. Abstaining from alcohol at any stage of liver disease is associated with a reduced liver-related mortality (5, 6). This raises the need of public health policies with the aim of reducing alcohol consumption in the community. Current guidelines suggest three different approaches, namely price-based policies, reduction of alcohol affordability and marketing and advertisement bans, to reduce liver-related mortality, effectively (2).

1.2 Clinical management of ALD

The clinical management of ALD, especially in early compensated stages, remains challenging. Few studies have investigated early stages of ALD. Results from several studies indicate that most ALD patients are diagnosed with advanced disease when severe clinical symptoms are evident (5–9).

1.2.1 Clinical diagnosis of ALD

1.2.1.1 Early ALD

Patients in early stages of ALD are often asymptomatic and even have normal laboratory findings (2). In reasonable numbers of cases only signs of alcohol use disorder (AUD) are present, e.g. hypertrophy of the parotid gland, malnutrition, peripheral neuropathy or Dupuytren's contracture. As the disease advances laboratory abnormalities and clinical signs of hepatitis occur frequently (10).

Patients with clinical suspicion of ALD should undergo screening for AUD by the Alcohol Use Disorder Identification Test (AUDIT). The Questionnaire consists of ten items comprising the categories of alcohol consumption, drinking behaviour and alcohol-related problems. Each item is assigned 0 to 4 points, for a maximum score of 40. Eight points or higher are associated with a high incidence of AUD (11). The AUDIT shows good validated psychometric characteristics and is easy for primary health care personnel to use (12–17). Patients with a score higher than eight should be further evaluated for liver injury with laboratory tests (18). Screening for ALD should not consist only of laboratory evaluation for liver function. Evidence exists that patients with advanced fibrosis can have normal blood work results, so that evaluation for liver fibrosis with transient elastography (TE), e.g., is indicated (2).

TE is a bed-side tool for the assessment of liver fibrosis by measuring liver stiffness in terms of sound waves. Thiele et. al. (19) showed in a prospective study that elastography is very accurate in predicting liver fibrosis. According to this study TE also can rule out cirrhosis. Voican et. al. (20) also demonstrated the excellent diagnostic value of TE in assessing liver fibrosis. They also showed in their study, that the combination of TE and serum markers for fibrosis is not superior to TE alone in diagnosing fibrosis.

In addition, Singal, et. al. (18) recommend for patients with AUD that counselling by hepatologists should be supported by addiction specialists.

1.2.1.2 Alcoholic hepatitis (AH)

Patients with AH characteristically present with jaundice of acute onset, fever, ascites and proximal muscle loss and as well as in severe cases hepatic encephalopathy (21).

Lucey, Mathurin and Timothy (21) proposed that establishing the diagnosis of AH specific laboratory findings, clinical signs of liver failure and a patient history of heavy alcohol intake.

Elevated aspartate aminotransferase (AST) activity, a ratio of AST to alanine aminotransferase (ALT) activity higher than 2, an elevated total serum bilirubin value, as encountered with jaundice, an elevated Internationalized Ratio (INR) value and neutrophilia in combination with ascites should lead to the diagnosis of AH. Moreover, common entities in the differential diagnosis should be evaluated. These include the evaluation of patient history for exposure to drugs or other xenobiotic agents in the last three months, screening for bleeding and infection, especially spontaneous bacterial peritonitis and urinary tract infections with exclusion by serologic studies of a superimposed infection with a hepatotropic virus, e.g. hepatitis virus A, B or C. (21–23).

1.2.2 The role of liver biopsy in clinical management

The EASL Clinical Practice Guidelines: Management of Alcohol-Related Liver Disease 2018 (2) recommend liver biopsy in phase II and larger phase III clinical trials and in selected patients, when non-invasive tests are inconclusive or there is suspicion of co-existence of aetiologies.

For establishing the diagnosis of AH a liver biopsy is not routinely needed (21).

1.2.3 Therapeutic options

The fundamental pillar in the treatment of alcoholic liver disease independent of the amount of liver damage is abstinence. Lackner et. al. (6) demonstrated, that abstinence is an independent predictor of long term survival in ALD. Therefore each patient should see an addiction specialist managing the AUD (18, 21).

The treatment of ALD however, remains challenging.

1.2.3.1 Clinical scores for assessing the severity of ALD

Three different scores are routinely in clinical use to predict the short-term prognosis for patients with severe AH and to support treatment decisions such as the use of corticosteroids. They are, Maddrey's discriminant function (MDF), the Model of End Stage Liver Disease (MELD) and the Lille Score (21).

MDF values are calculated from prothrombin time and serum bilirubin level:

$$DF = 4{,}6 * prothrombin\ time\ (sec) + serum\ bilirubin\ (mg\ per\ dl) \quad (24)$$

An MDF higher than 32 indicates severe AH and supports the administration corticosteroids (24).

The MELD-score was designed for predicting mortality in patients awaiting liver transplantation and is based on serum levels of bilirubin and creatinine and on the INR (21).

$$MELD\ Score = 9.57 * \ln\big(creatinine\ (mg\ per\ dl)\big) + 3.78 * \ln\big(bilirubin\ (mg\ per\ dl)\big) + 11.2 * \ln(INR) + 6.43) \quad (25)$$

Dunn et. al. (25) pointed out, that the MELD score is as adequate as the MDF in predicting short-term survival in patients with clinical AH and suggested a score of 21 and higher as an optimal cut-off for initiating adequate treatment.

The Child-Pugh-Score is used for clinical staging of cirrhosis independent of aetiologies and predicts 1-year survival. Table 1 shows the grading criteria.

Table 1: Child-Pugh-Score (CPS) grading criteria adapted from Pugh et. al. (26)

Parameters	Points scored for increasing abnormality		
	I	II	III
Encephalopathy (grade)	none	1 and 2	3 and 4
Ascites	absent	slight	moderate
Bilirubin (mg per dl)	1-2	2-3	>3
Albumin (g per dl)	>3.5	2.8 – 3.5	<2.8
Prothrombin time (sec)	1-4	4-6	>6

Based on this score patients are divided into three subgroups (CPS A, CPS B, CPS C) with 1-year mortality rates of 29%, 38% and 88% respectively (26).

Louvet et. al. (27) developed a model to predict the effectiveness of corticosteroids. The score devised (the Lille score) is based on age, serum bilirubin, creatinine and albumin and prothrombin time at day 0 and serum bilirubin after seven days.

The authors propose stopping the administration of cortidecosteroids after 7 days for patients with a score higher than 0.45 (27).

1.2.3.2 Corticosteroids

Currently available clinical practice guidelines propose the administration of 40 mg per day of prednisolone for 4 weeks in patients with an MDF exceeding 32 or a MELD-score above 21 (18, 22).

Corticosteroid treatment should be evaluated and possibly terminated by using the Lille model (see above).

Approximately 40% of patients with alcoholic hepatitis do not respond to prednisolone. Unfortunately there is no adequate alternative treatment option (21).

1.2.3.3 Pentoxifylline

Akriviadis et. al. (28) showed in a double-blind randomized trial, that the administration of 400 mg pentoxifylline for 28 days improved short-term survival in severe AH.

The so-called STOPAH-trial evaluated the administration of pentoxifylline and corticosteroids in relation to survival at 90 days and one year. Unfortunately, in contrast with the results of Akriviadis et. al., there was no survival benefit in the pentoxifylline group (29). Therefore, also according to the current EASL Guideline: Management of Alcoholic-Related Liver Disease the use of pentoxifylline is discouraged (2).

1.2.3.4 Nutritional support

Malnutrition and sarcopenia are very frequently encountered in patients with alcoholic hepatitis (18, 21, 22) and have been considered makers of adverse prognosis. However, the data on the utility of enteral and parenteral nutritional support are controversial (18). Cabré et. al. (30) compared administration of corticosteroids with enteral nutrition in a randomized trial and showed, that short-term survival was similar in both groups. Nevertheless, current guidelines suggest

the intake of 35-40 kcal/kg of body weight and a daily protein intake of 1.2-1.5 g/kg of body weight. Oral nutrition is considered the first-line approach (2).

1.3 Morphologic features of alcohol-related liver disease

Alcohol-related liver disease (ALD) comprises a broad spectrum of morphologic entities including alcohol-related steatosis, steatohepatitis due to alcohol (ASH) and alcohol-related fibrosis/cirrhosis (10).

1.3.1 Alcohol-related steatosis

Generally, alcohol-related steatosis of the liver is defined as an accumulation of lipid droplets in hepatocytes. Two types can be distinguished, macrovesicular and microvesicular steatosis (31).

The macrovesicular type is recognized by large lipid vacuoles, larger than the nucleus, that may displace the nucleus to the periphery of the hepatocellular cytoplasm. The lipid droplets are enclosed in a membrane containing phospholipids and proteins. On the contrary, in microvesicular steatosis the hepatocellular cytoplasm is filled with and expanded by minute lipid droplets without membranes and the nucleus stays in central position within the cytoplasm (31).

It is also possible to see both patterns of fatty change together, a so-called mixed pattern. Yip and Burt reported a higher likelihood of progression to advanced ALD in mixed-pattern disease than in cases with purely macrovesicular steatosis (31).

In the histopathologic assessment of liver biopsies, the amount of steatosis is estimated semi-quantitatively by the percentage of parenchyma containing fat vacuoles. It is categorized as absent if fewer than 5% of hepatocytes contain macrovesicular fat and as mild if the percentage is between 5 and 33%, intermediate if the extent is between 33 and 66% and severe if it is above 66% (32).

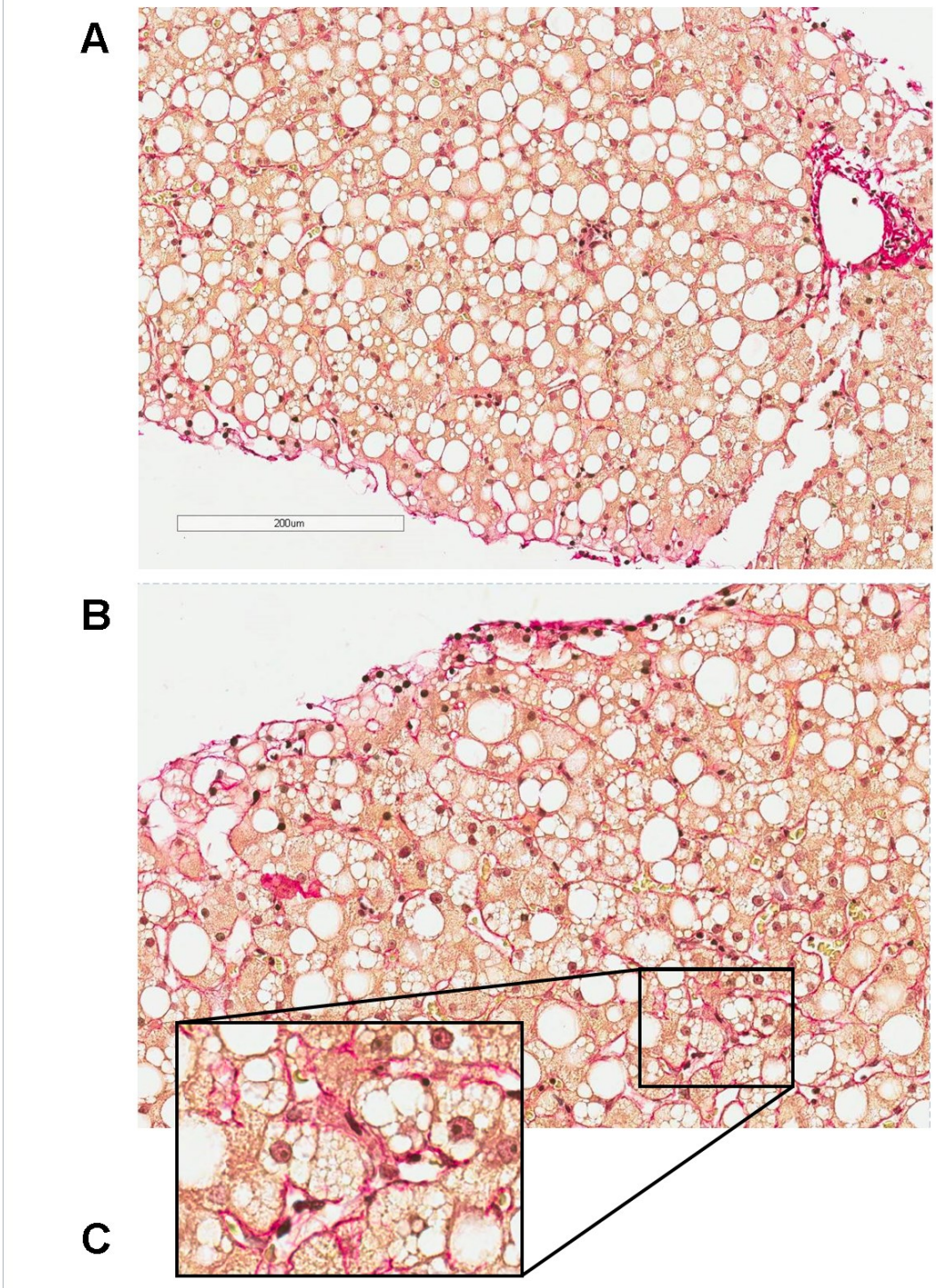

Figure 1: Alcohol-related steatosis: (A) Macrovesicular steatosis, which is recognized by large lipid vacuoles, larger than the nucleus, that may displace the nucleus to the periphery of the hepatocellular cytoplasm; (B) In microvesicular steatosis the hepatocellular cytoplasm is filled with and expanded by minute lipid droplets without membranes and the nucleus stays in central position within the cytoplasm; (C) Mixed pattern, contains both macrovesicular and microvesicular steatosis, simultaneously
(biopsy specimen, Sirius red stain)

1.3.2 Steatohepatitis due to alcohol (ASH)

Steatohepatitis is defined by three key morphological features: steatosis, hepatocellular ballooning and lobular inflammation. Other morphological changes frequently encountered include Mallory-Denk bodies (MDB), hepatocellular necrosis, fibrosis and cholestasis (31). These histological features are not necessarily accompanied by clinical symptoms and therefore ASH must be distinguished from the clinical syndrome of AH. This clinical syndrome is defined (see above) as acute onset of jaundice and clinical signs of liver failure after years of marked alcohol abuse (21).

The morphologic changes of ASH are predominantly located in acinar zone 3 in the precirrhotic stages of disease (33).

Hepatocellular ballooning is defined as cell swelling, rounding and clarification with wispy cytoplasm (34). It must be distinguished from macrovesicular steatosis (31). Moreover, in ballooning degeneration MDB are regularly present. Lackner et. al. (35) showed that ballooned hepatocytes exhibit severe decrease or even loss of cytoplasmatic marking for keratin 8 /18 on immunostaining. This reflects reorganization of the intermediate filament cytoskeleton that is composed of keratin 8 and 18 proteins, and is ascribed to increased oxidative stress.

MDB consist mainly of aggregated keratin 8 and 18 proteins with P62 protein and ubiquitin (31). In H&E stained material MDB are strongly eosinophilic hyaline appearing irregular inclusions in the hepatocellular cytoplasm (34). Immunostaining for keratin 8/18, P62 and ubiquitin may help to detect small inclusions of this type and can be used to identify MDBs (31, 34, 36).

Another light-microscopic finding in the context of hepatocyte damage in steatohepatitis is that of mega-mitochondria. These are defined as eosinophilic globular or needle shaped eosinophilic cytoplasmic inclusions of approximately 2 to 10 µm in diameter. They are red in material stained with chromotrope-aniline blue (CAB) (34). However, megamitochondria are not specific for ALD, they also are seen in other liver diseases.

Lobular inflammation of variable extent is seen in ASH. The inflammatory infiltrate consists mainly of neutrophils but may also contain mixed lymphocytes and histiocytes. This infiltrate is centred on ballooned hepatocytes (31, 34).

Another feature of steatohepatitis due to alcohol is the presence of fibrosis, which as mentioned above is, like the other key features of ASH, most pronounced in acinar zone 3.

During the evolution and progression of ALD, different types of fibrosis may occur. In alcohol-related steatosis perivenular fibrosis may be seen, which is defined by Nakano et. al. (37) as thickening of at least 75% of the perimeter of the wall of the central vein. In connection with perivenular fibrosis the patients can develop obliteration of the terminal hepatic vein (THV), so-called phlebosclerosis, which is thought to be responsible for precirrhotic portal hypertension (31). Central hyaline necrosis is defined by Edmondson et. al. (38) as fibrosis, fibro-obliterative changes and hepatocyte necrosis with MDB around the THV. It represents the severest form of changes among those involving the THV (31, 33). Another type of connective tissue deposition is pericellular and perisinusoidal fibrosis (PCF). It is defined as collagen deposition around ballooned hepatocytes. The cells are practically immured by the connective tissue. The pericellular pattern resembles that of wire mesh used for small-animal pens, with hepatocytes lying in the interstices among wires, and the term “chicken-wire fibrosis” has been employed (34). PCF initially occurs mainly around THV and within adjacent parenchyma. As fibrosis progresses PCF begins to link THV with portal tracts as well as THV with THV. As hepatocytes in regions affected by this form of fibrosis are lost, stroma condenses. The formation of septa begins, which, if alcohol abuse continues, ends in alcoholic cirrhosis (33).

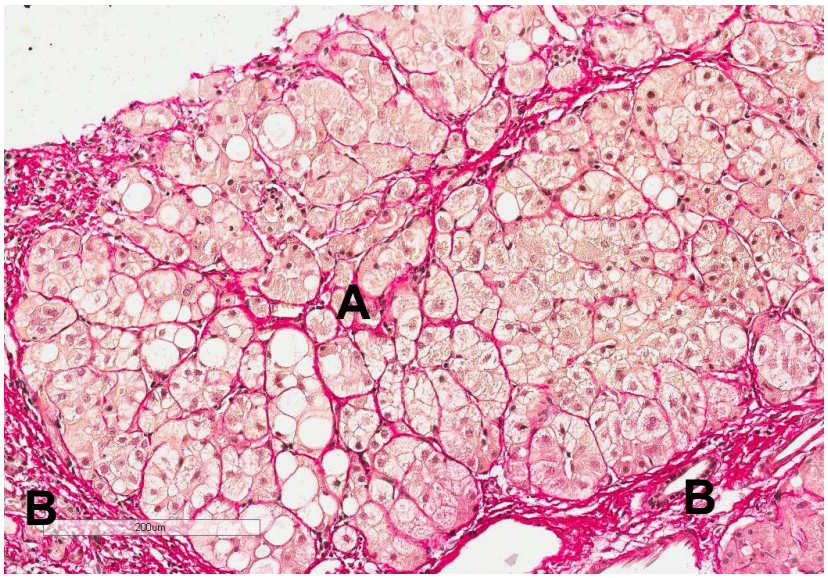

Figure 2: (A) Pericellular fibrosis, defined as collagen deposition around ballooned hepatocytes. The cells are practically immured by the connective tissue. **(B) Septal fibrosis,** defined as strands of connective tissue linking terminal hepatic venules (THV) and portal tracts or THV with THV (biopsy specimen, Sirius red stain)

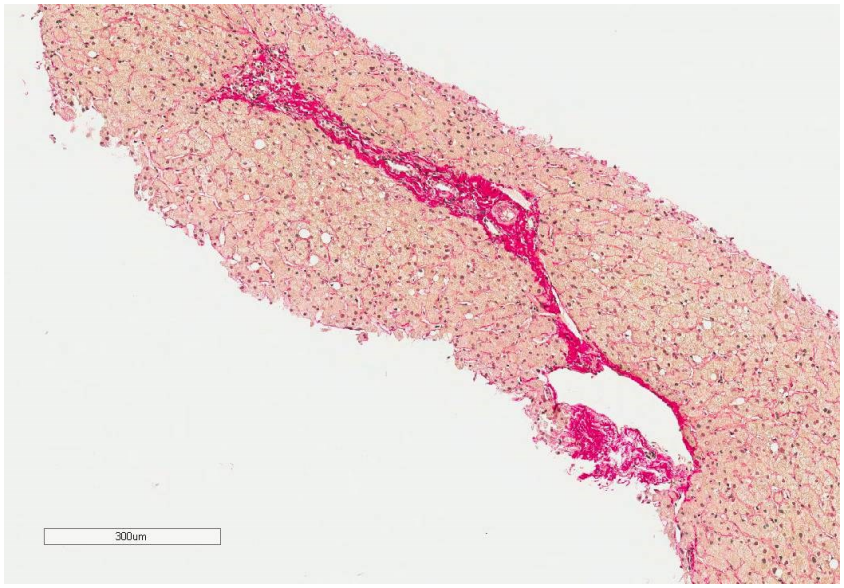

Figure 3: Septal fibrosis: is characterized by thicker strands of connective tissue. The strands as they develop undergo loss of incorporated hepatocytes (biopsy specimen, Sirius red stain).

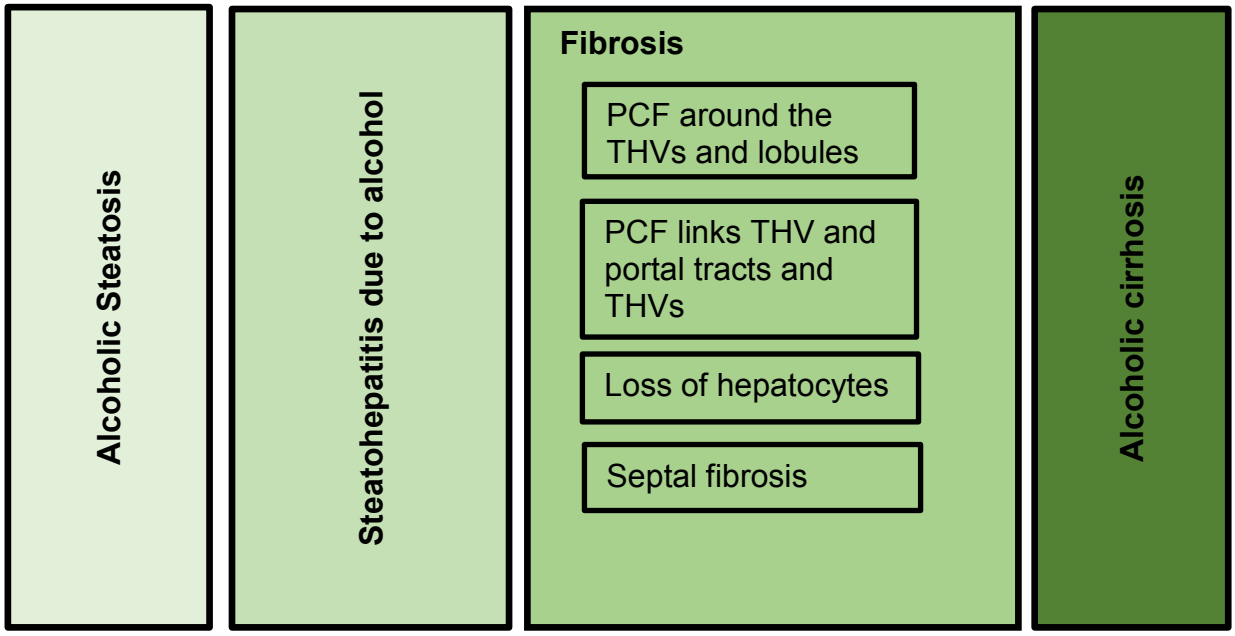

Figure 4: Progression of morphological features in ALD: Alcohol abuse initially leads to steatosis of hepatocytes. This can be accompanied by hepatocellular ballooning and lobular inflammation (steatohepatitis due to alcohol). With disease progression changes to the THV occur, such as perivenular fibrosis, phlebosclerosis and central hyaline necrosis. The fibrosis progresses with a pericellular pattern into lobular areas and eventually links THV and portal tracts or THV with THV. Due to hepatocyte loss in those areas densely fibrotic septa develop, which finally ends in full-blown alcoholic cirrhosis. (33)

1.3.3 Alcoholic cirrhosis

Anthony et. al. (39) define cirrhosis as a diffuse process characterized by fibrosis and the conversion of normal liver architecture into structurally abnormal nodules. According to that definition nodularity and fibrosis can be seen as fundamental criteria for diagnosing cirrhosis on morphologic grounds. Other histologic features also indicate that cirrhotic destruction of the normal architecture has occurred. These include two cell layer thick trabecular structure, distortion of vascular architecture, hepatocellular changes and fragmentation of biopsy-specimen tissue (34). Cirrhosis can be subclassified, based on the macroscopic appearance of the nodules, into marcronodular, micronodular and mixed cirrhosis (39).

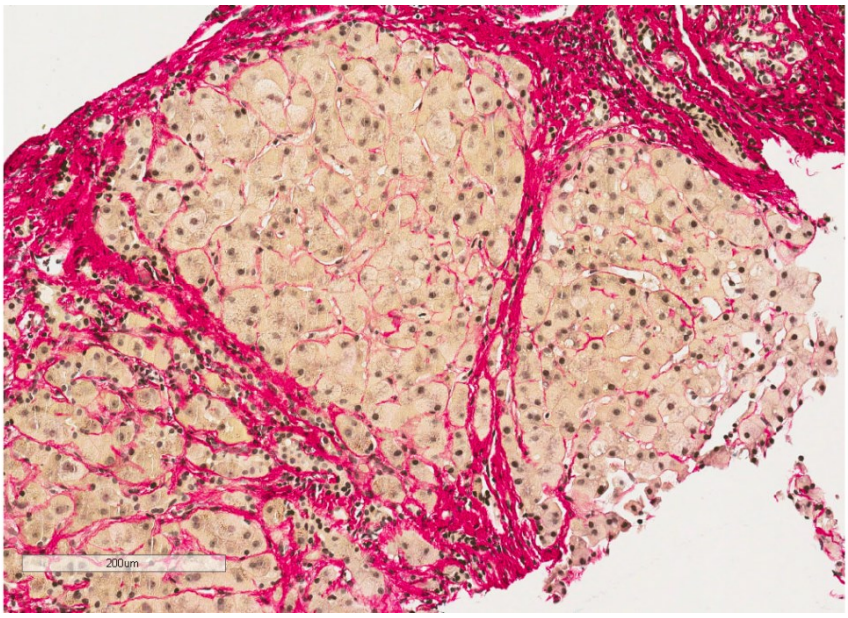

Figure 5: Alcoholic cirrhosis: Cirrhosis is defined as a diffuse process characterized by fibrosis with the conversion of normal liver architecture into structurally abnormal nodules. (biopsy specimen, Sirius red stain)

With reticulin staining, abnormality in structure can be demonstrated in the form of malorientation of reticulin fibres. Moreover, the number of portal tracts decreases in proportion to number of THV and septa, that link terminal veins and portal tracts, are regularly seen (34).

In a cirrhotic liver, two additional hepatocellular changes can be observed: First, there is histologic evidence of hepatocellular regeneration with the morphologic correlate of thickening of liver-cell-plates and loss or rarefication of lipofuscin pigment. Another very characteristic feature is pleomorphism, which is defined by the presence of adjacent populations of hepatocytes growing at different rates and having different cell and nuclear characteristics.

In some cirrhotic livers evidence of dysplasia can be seen. This includes large-and small-cell-dysplasia or large-cell-change and small-cell-change, respectively (34).

The differential diagnosis of cirrhosis includes nodular regenerative hyperplasia, focal nodular hyperplasia and a well-differentiated hepatocellular carcinoma (34).

In some cirrhotic livers the cause can be ascertained by typical histologic features alone. However in most cases the medical history must be considered. Lefkowitch (34) proposes a scheme for the assessment of the aetiology (see Table 2).

Table 2: Morphologic features for cause assessment (adapted from Lefkowitch (34))

Morphologic features for cause assessment
Pattern of nodules and fibrosis
Bile ducts
Blood vessels
ASH
Evidence of viral infection
Abnormal deposits
Iron
Copper
α_1-Antitrypsin globules

1.3.3.1 Assessment of histologic activity and stage

Unlike in non-alcoholic fatty liver disease (NAFLD) no semiquantitative scoring system permits assessment of inflammatory activity (grade) and degree of fibrosis and destruction of lobular architecture (stage) in alcoholic cirrhosis. Yip and Burt (31) propose use of the scoring system of the Non-alcoholic Steatohepatitis Clinical Research Network described by Kleiner, et. al. (32). However, significant clinical and histological differences between those two diseases may impair the utility of such an approach.

1.3.4 Hepatocellular carcinoma (HCC)

Cirrhosis precedes the development of most instances (70 to 90%) of hepatocellular carcinoma (HCC) in the western world (40). Approximately 15 % of patients with alcoholic cirrhosis develop HCC. This rate increases with the presence of cofactors such as hepatitis-C-virus infection, hepatitis-B-virus infection and the exposure to aflatoxin B (2, 40). Mancebo et. al. (41) showed in a prospective study among 450 CPS A and B patients with ALD that the annual incidence of HCC is about 2.6% and that age and low platelet count are independent risk factors. On the contrary, cessation of alcohol abuse is thought to reduce HCC development by about 6 to 7% annually (42).

Morphologic features, that are thought in macroregenerative nodules in cirrhosis to mark progress toward HCC are, for example, small-cell-change, loss of reticulin framework and prominent MDB.

Lefkowitch (34) coined the term dysplastic focus, which means a cluster of hepatocytes with signs of small- or large-cell dysplasia. Watanabe et. al. (43) first described small-cell-dysplasia as cells, which are smaller, than hepatocytes but larger than cancerous cells. Moreover, they show nuclear pleomorphism, multinucleation and cytoplasmic basophilia (44). Large-cell-dysplasia, first described by Anthony et. al. (45), is defined as cellular enlargement, nuclear pleomorphism and multinucleation of cell-groups in cirrhotic livers. Many studies demonstrated an increased risk of HCC associated with two histologic findings (46–48).

HCC can be distinguished from regenerative nodules by plate architecture, reticulin pattern, cellular characteristics and siderosis. The architecture appears more abnormal, reticulin fibres are absent, the cells show typical malignant features and siderosis is absent, unlike to cirrhosis (34).

Table 3: Differential diagnosis of hepatocellular carcinoma (HCC) in alcoholic cirrhosis (34, 40)

	HCC	Dysplastic nodule	Regenerative nodule
Plate Architecture	trabecular, pseudoglandular, sccirrhous	atypical architecture, focal pseudoglandular structures	two or three cells-thick layers, no distortion in plate-arrangement
Reticulin pattern	scanty or absent	focal loss	normal
Cellular characteristics	pleomorphism, clear cells, sarcomatous change, bile production, MDBs, ground glass inclusions	small-cell-dysplasia, large-cell-dysplasia, increased cellularity	no typical malignant features, MDBs
Siderosis	not present		present

1.4 Alcoholic metabolism and pathogenesis of liver injury in ALD

There are three different pathways for the metabolism of alcohol in humans: the alcohol dehydrogenase (ADH) pathway, the microsomal ethanol-oxidizing system (MEOS) pathway and the catalase pathway (49, 50).

ADH oxides ethanol with the cofactor nicotinamide adenine dinucleotide (NAD) to acetaldehyde. The factor limiting this reaction is the availability of NAD through regeneration, which in chronic alcohol abuse is insufficient. The most accelerated pathway in chronic alcohol abusers is the MEOS pathway, including the enzyme cytochrome P-450 2E1, which undergoes increased activation in this context. The catalase pathway eliminates ethanol in peroxisomes by oxidation and combined reduction of hydrogen peroxide (49, 50).

The enzymes involved are mostly located in centilobular regions rather than in periportal zones. This has been invoked to explain why the lesions of ALD affect principally acinar zone 3 (33).

In chronic alcohol abuse the metabolizing pathways are accelerated, which leads to oxidative stress (catalase pathway), accumulation of acetaldehyde (ADH pathway) and mitochondrial damage (MEOS pathway). Is consequence Kuppfer cells are activated directly. Hepatic inflammation and translocation of gut microbes caused by acceleration of those pathways (33, 50)

Activated Kupffer cells produce growth factors and chemokines that encourage hepatic stellate cells to produce extracellular matrix and to express α-smooth muscle actin, which leads to a massive production of extracellular matrix and this is the main cause of liver fibrosis (33, 51).

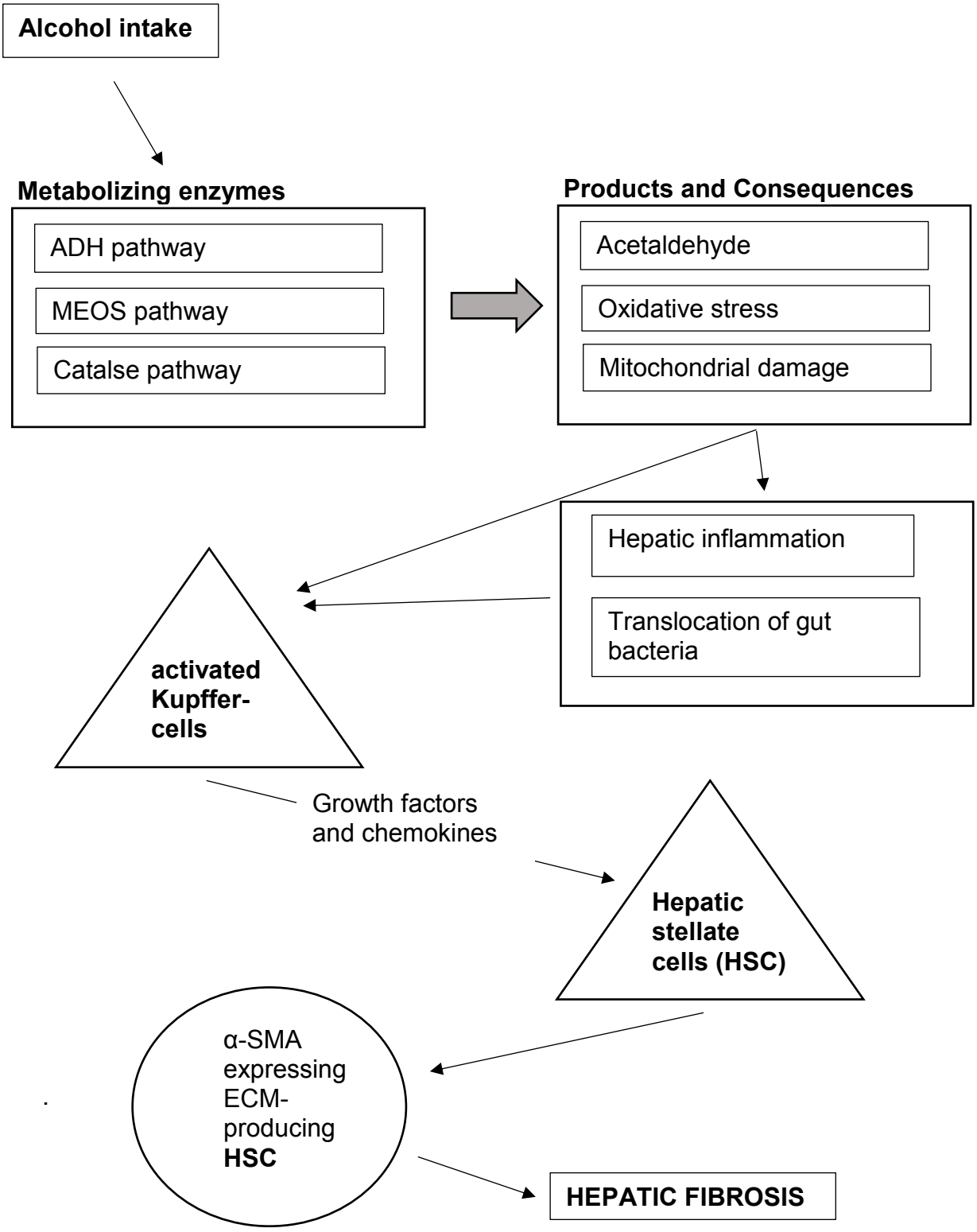

Figure 6: Pathophysiology of liver fibrosis in excessive alcohol intake: An acceleration of the three main alcohol metabolizing pathways leads to increased liver inflammation, translocation of gut microbes, and activation of Kupffer cells. These secrete growth factors and chemokines that activate hepatic stellate cells. (33, 50, 51)

2 Objectives

The objective of this study was to evaluate the pericellular fibrosis compared with septal fibrosis as a marker of long-term prognosis in patients with high stage ALD. Researchers have not yet quantitatively differentiated in this setting connective tissue according to its morphological patterns. Lackner et. al. (6) showed semi-quantitatively that fibrosis of the pericellular pattern a single predictor of long-term survival with a tendency to favourable patient outcome in clinically decompensated patients. To overcome the limitations of a semi-quantitative analysis we evaluated the two different morphological features with a morphometric algorithm.

This differentiation of pericellular and septal fibrosis was expected to yield a deeper understanding of possible survival differences between those two classes of patients. It was hoped that the results might provide insight into mechanisms for any difference and to generate hypothesis that could be explored in further studies.

3 Aims

To achieve the above-mentioned objectives, we investigated 192 patients with ALD, who underwent liver biopsy in the Department of Gastroenterology and Hepatology of the Medical University of Graz.

To assess the stage of ALD the CRN staging system and the Laennec score were used. Patients were stratified according to CRN stage and to clinical disease compensation.

To quantify connective tissue for different fibrosis types separately, the tissue sections stained with Sirius red were scanned. Lobular areas were marked according to exact definitions. Both the annotated lobular regions and the tissue overall were analysed using morphometric analysis software.

Based on the measured amounts of connective tissue and non-classified tissue, the overall CPA, the septal CPA, the pericellular CPA, the PPA, the proportion of pericellular to septal CPA were calculated by defined formulas.

The measurement of steatosis was performed with the same morphometric analysis software.

In order to correlate the measured morphologic features with clinical outcome, all subjects were followed until death or until liver transplantation.

To investigate mechanisms contributing to different types of fibrosis, these parameters were correlated with clinical-laboratory test results as determined at the time of liver biopsy.

4 Patients and Methods

4.1 Patients

In this retrospective study 192 patients (female: 57) with ALD, who underwent either percutaneous or transjugular liver biopsy between 1995 and 2009 at the Department of Gastroenterology and Hepatology of the Medical University of Graz (MUG) were assessed.

This study was approved by the ethics committee of the Medical University of Graz (20-414 ex 08/09).

Patients had either early compensated ALD or decompensated ALD. Compensation is defined by a serum bilirubin value higher than 3 mg/dl without clinical signs of decompensation, such as ascites or encephalopathy.

Biochemical-study results and clinical details were collected from medical charts.

All patients were followed until death or censored with data from the liver clinic. Those who underwent liver transplantation were censored with transplantation date.

4.2 Routine stains

Formalin-fixed liver biopsy cores were embedded in paraffin and microtome-sectioned at 3 µm. For evaluation of inflammation and hepatocellular damage one section was stained with hematoxylin and eosin (H&E). Another was stained with Sirius red used to identify collagen fibers. Both stains employed standard procedures.

4.3 Histologic staging

The Laennec score and the CRN staging system were used to assess the histologic stage of fibrosis.

4.3.1 Assessment of Laennec stage

The following table gives an overview of the Laennec scoring system proposed by Kutami et al. (52), which divides patients in the cirrhotic stage into three different categories (see Table 4).

Table 4: Laennec scoring system adapted from Kutami et. al. (52)

Stage	Name	Septa (thickness and number)	Criteria	Score
0	No definite fibrosis			0
1	Minimal fibrosis	+/-	No septa or rare thin septum; may have portal expansion or mild sinusoidal fibrosis	1
2	Mild fibrosis	+	Occasional thin septa; may have portal expansion or mild sinusoidal fibrosis	2
3	Moderate fibrosis	++	Moderate thin septa; up to incomplete cirrhosis	3
4A	Cirrhosis, mild, definite, or probable	+++	Marked septation with rounded contours or visible nodules. Most septa are thin (one broad septum allowed)	4
4B	Moderate cirrhosis	++++	At least two broad septa, but no very broad septa and less than half of biopsy length composed of minute nodules	5
4C	Severe cirrhosis	+++++	At least one very broad septum or more than half of biopsy length composed of minute nodules (micronodular cirrhosis)	6

4.3.2 Assessment of non-alcoholic fatty liver disease (NAFLD) Clinical Research Network (CRN) stage

Kleiner et. al. proposed a staging system for fibrosis for patients with NAFLD, but it is widely used for ALD since no valid scoring system exists specifically for ALD patients (see Table 5).

Table 5: non-alcoholic fatty liver disease (NAFLD) CRN staging adapted from Kleiner et. al. (32)

Definition	Stage
None	0
Perisinusoidal or periportal	1
Mild, zone 3, perisinusoidal	1A
Moderate, zone 3, perisinusoidal	1B
Portal/periportal	1C
Perisinusoidal and portal/periportal	2
Bridging fibrosis	3
Cirrhosis	4

4.4 Digital image analysis (morphometry)

Digital image analysis is defined as a method for computer-assisted quantification of morphologic features of scanned tissue sections (53). In our study, we used Definiens Developer XD 2.6.0 Build 54490 x64 (Definiens®, Munich Germany) to evaluate the amount of connective tissue and to analyse pericellular and septal fibrosis separately. Macrovesicular steatosis also was quantified.

The Sirius red stained biopsy sections were scanned with an Aperio ScanScope (Leica Biosystems Nussloch GmbH, Nussloch Germany) with a magnification of 400x.

4.4.1 Septal differentiation

The Aperio ImageScope V 12.3.0.5056 (Leica Biosystems Nussloch GmbH, Nussloch Germany) was used to differentiate septal and pericellular fibrosis. Areas with fibrosis of the pericellular pattern were marked with annotations (particular names given individual parts of scanned images) for separate analysis in Definiens Developer XD Tissue Studio (Figure 7).

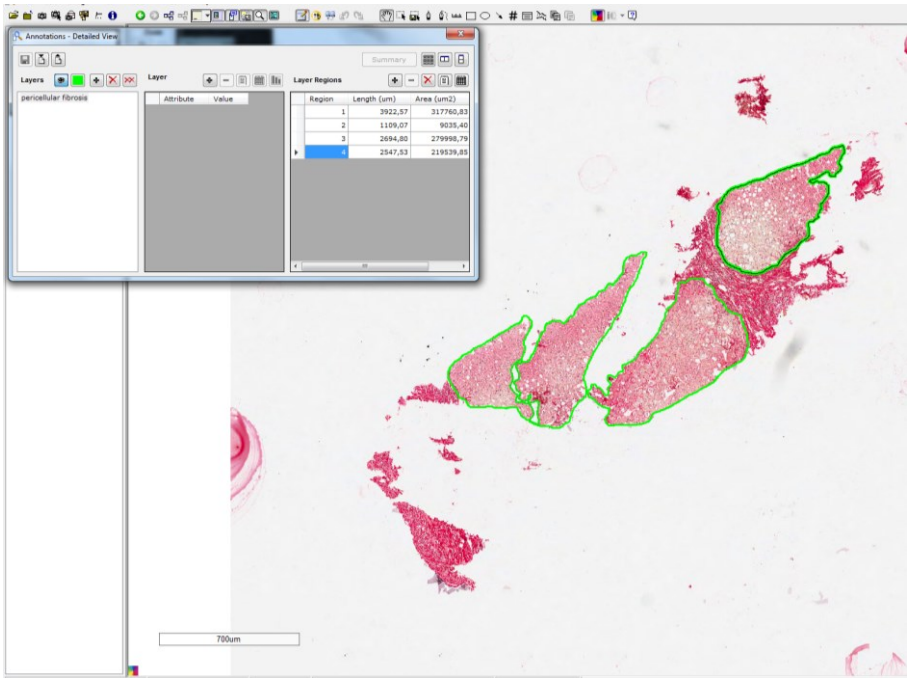

Figure 7: Septal differentiation: Annotations in Aperio Image Scope. The green-marked areas are considered to be sites of pericellular fibrosis (lobular area) and are analyzed individually. The remaining connective tissue is subsumed under septal fibrosis.

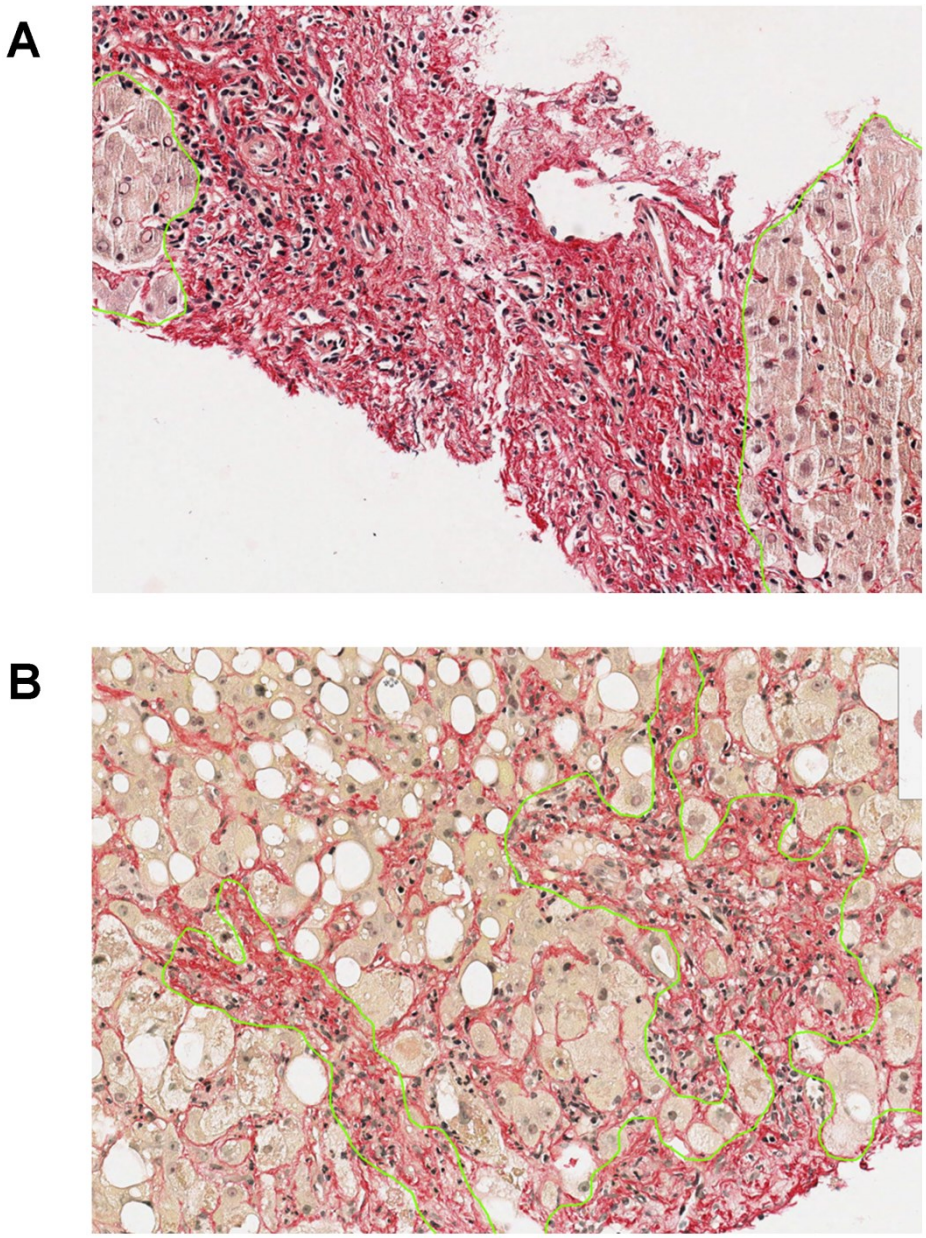

Figure 8: Septal differentiation: (A) Marked septal fibrosis, low pericellular fibrosis; (B) Low septal fibrosis, marked pericellular fibrosis

As no agreed, consistent and validated definition of septal fibrosis in cirrhotic livers exists, we defined a septum as an area of fibrotic tissue of which less than 10% consisted of hepatocytes. Furthermore, areas with portal structures, i.e. bile ducts, arterial or portal vein branches, and ductular reaction were considered as septal. To avoid an overestimation of septal and overall fibrosis parts containing liver capsule were excluded from the analysis (Figure 8).

Therefore the following areas were defined and measured:

- Area within marked annotations (lobular area)

- Area of the entire biopsy (overall area)

All biopsies were assessed at a magnification of 200x and with supervision by an expert pathologist.

4.4.2 Collagen proportionate area (CPA)

We used Definiens Developer XD to assess of the amount of connective tissue.

The extent of fibrosis is quantified by the collagen proportionate area, which is defined as the ratio of the area identified as connective tissue by morphometry to the whole analysed area (53).

Quantification of connective tissue is based on the measurement of areas of a certain colour at a defined threshold of intensity of staining. Taking collagen as an indicator of fibrosis, we marked fibrosis using Sirius red staining, which colours collagen red.

The threshold selection was defined on the basis of published work, with close supervision by an expert pathologist and was comparable throughout all biopsies. A few modifications were necessary due to different staining intensities in different biopsy specimens. Structures with abundant connective tissue, especially in bigger septa, may contain, e.g., bile ducts or inflammatory cells. Those were not part of the measurement and excluded either by different colour intensity or by nuclei identification with cell simulation and exclusion.

After final review of small tissue sections at random data were collected and areas are calculated (Figure 9, Figure 10)

CPA variables were assessed with these formulas:

$$overall\ CPA = \frac{fibrosis\ in\ overall\ area\ (\mu m^2)}{overall\ area\ (\mu m^2)}$$

$$pericellular\ CPA = \frac{fibrosis\ in\ lobular\ area\ (\mu m^2)}{overall\ area\ (\mu m^2)}$$

$$septal\ CPA = \frac{fibrosis\ in\ overall\ area\ (\mu m^2) - fibrosis\ in\ lobular\ area\ (\mu m^2)}{overall\ area\ (\mu m^2)}$$

$$proportion\ of\ septal\ CPA\ to\ pericellular\ CPA = \frac{septal\ CPA}{pericellular\ CPA}$$

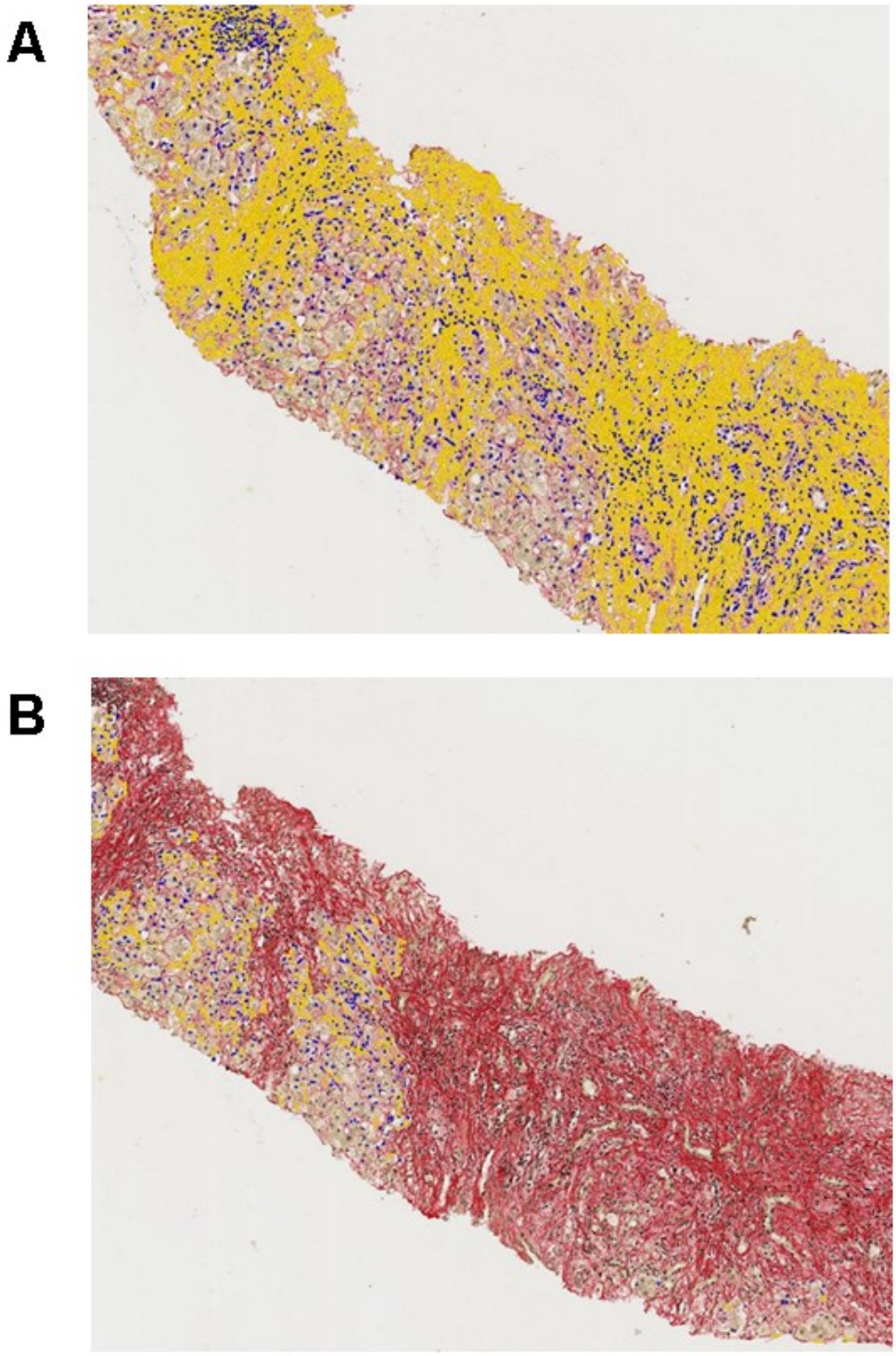

Figure 9: Collagen proportionate area (CPA) assessment: (A) The yellow area is the amount of collagen tissue classified by morphometry in the overall area. (B) In contrast to A, the yellow colour marks the connective tissue in the lobular area.

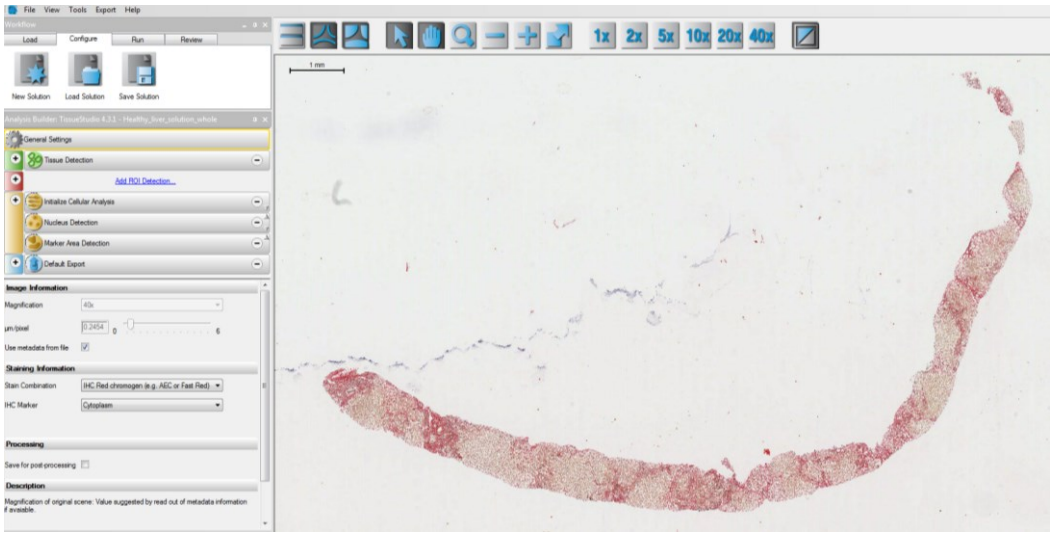

Figure 10: CPA-algorithm: The morphometric algorithm consists of background separation, tissue detection, marker area classification and calculation of the area of connective tissue. The algorithm is applied to lobular area and overall area separately.

4.4.3 CPA in healthy liver

To identify the marker threshold, we had to consider physiologic CPA values in a healthy liver, in order not to overestimate the connective tissue in cirrhotic livers.

In a pilot study, we evaluated overall and parenchymal CPA from one liver resection specimen classified as healthy by an expert pathologist. Sections of liver biopsied virtually in Aperio ImageScope using annotations described. The biopsies were considered to be representative with a length of 1,6 mm and a width of 1,2 mm containing 15 portal tracts at least.

The separate measurement of the parenchymal and perivenular areas is due to a differentiation of pericellular and septal fibrosis in the main study. The portal tracts are marked with annotations in a different layer than the biopsy with 20x-magnification.

4.4.4 Parenchymal proportionate area (PPA)

The PPA is defined as the proportion of non-fibrotic tissue to all analysed tissue, which means the regions occupied by hepatocytes.

The PPA is calculated as following:

$$PPA = \frac{lobular\ area\ (\mu m^2) - fibrosis\ in\ lobular\ area(\mu m^2)}{overall\ area\ (\mu m^2)}$$

4.4.5 Steatosis

Generally, the assessment of steatosis is performed semiquantitatively. The pathologist estimates the amount of steatosis in relation to the parenchyma and categorizes the percentage into three groups (<33%, 33-66%, >66%) (32).

The measurement was performed in Definiens Developer XD. In liver stained with Sirius red fat vacuoles occur as white/colourless, round and homogenous. These features distinguish fat from other white/colourless regions.

As a first step all white areas are marked and classified as fat vacuoles. Secondly, all features are compared for roundness, shape and homogeneity. Only those areas with features that fit into the defined cut-offs are retained as steatosis.

We defined steatosis by the area of fat droplets related to the parenchyma, which we achieved using the parenchymal area measured above.

$$Steatosis = \frac{area\ of\ classified\ fat\ vacuoles\ (\mu m^2)}{lobular\ area\ (\mu m^2) - fibrosis\ in\ lobular\ area\ (\mu m^2)}$$

4.5 Statistical analysis

Statistical analysis was performed for patients with histologically evident cirrhosis (NAFLD CRN stage 3 and 4) and for clinically compensated and decompensated patients (independent of CRN stage) separately.

Demographic, morphologic and biochemical data were graphed to display median and range. The compensated and decompensated groups were compared by non-parametric tests (Mann-Whitney-U).

For the morphometric variables, an optimal cut-off was estimated using the Youden-index. Liver-related mortality was calculated by Kaplan-Meier-analysis. Values were compared using the log-rank-test. A p-value under .05 was considered significant.

Correlation analysis of morphometric and clinical laboratory parameters was performed with Spearman's Rho.

5 Results

5.1 Study cohort

Participants (n=192) with ALD histopathologically diagnosed by an expert pathologist were included in this study. Those with other diagnoses, e.g., non-alcoholic liver disease, with malignancies, or whose liver biopsy specimens were insufficient for study were excluded from participation (Figure 11).

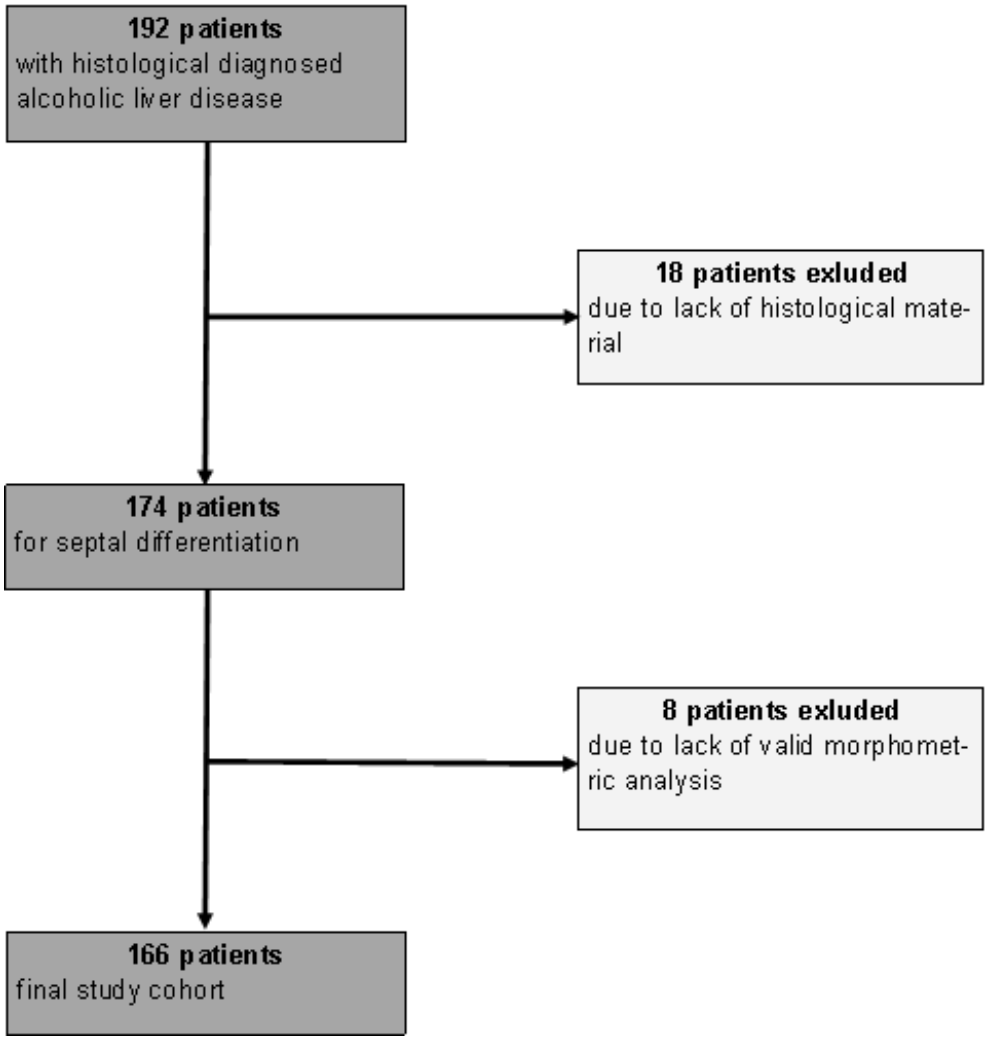

Figure 11: Study cohort

5.2 Clinical and biochemical characteristics

The following tables give a short summary of the clinical and biochemical characteristics of the study cohort and the distribution of the features in different groups (see Table 6 and Table 7).

Table 6: Clinical and biochemical characteristics (in patients with compensated and decompensated ALD)

	compensated n=50		**decompensated n=116**		
Age	48.92	(24 - 74)	49.15	(25 - 73)	p = 0.381
BMI	26.5	(16.4 - 36.3)	24.25	(11.6 - 42.0)	p = 0.107
Sex, female %	20		34		p = 0.048
AST	37	(6 - 254)	49	(10 - 267)	p = 0.082
ALT	41	(10 - 308)	25	(3 - 116)	p = 0.000
GGT	125	(15 - 2795)	148	(10 - 2942)	p = 0.518
AP	126	(43 - 254)	184	(49 - 770)	p = 0.000
Bilirubin	1,3	(0.0 - 2.9)	6.1	(0.4 - 81.1)	p = 0.000
INR	1.03	(0.86 - 1.50)	1.38	(0.89 - 3.71)	p = 0.000
Albumin	4.4	(2.7 - 5.9)	3.2	(2.0 - 4.8)	p = 0.000
Leukocyte count	5.8	(3.5 - 12.8)	7.5	(2.4 - 31.6)	p = 0.002
Platelet count	146	(41 - 364)	127	(39 - 576)	p = 0.079
GI bleeding %	0		31		p = 0.000
HE %	0		28		p = 0.000
Ascites %	0		61		p = 0.000
MDF	3	(0 - 33)	25	(0 - 154)	p = 0.000
Child-Pugh-score	5	(5 - 10)	9	(5 - 14)	p = 0.000
MELD score	9	(6 - 15)	18	(6 - 47)	p = 0.000
Survival (years)	6.9	(0.3 - 14.5)	2.9	(0.0 - 15.7)	p = 0.000
5-year-mortality %	16		45		p = 0.000

Table 7: Clinical and biochemical characteristics (in patients with CRN stage 3 and 4)

	F3/F4 n=139	
Age	49.77	(25- 75)
BMI	25.1	(11.6 - 42.0)
Sex, female %	32	
AST	48	(6 - 207)
ALT	26	(3 - 111)
GGT	150	(10 - 2942)
AP	171	(49 - 770)
Bilirubin	4.3	(0.3 - 81.1)
INR	1.35	(0.89 - 3.71)
Albumin	3.3	(2.0 - 5.2)
Leukocyte count	7.0	(2.8 - 31.6)
Platelet count	125	(39 - 558)
GI bleeding %	25	
HE %	23	
Ascites %	52	
MDF	24	(0 - 154)
Child-Pugh-score	9	(5 - 14)
MELD score	15	(6 - 47)
Survival (years)	3.2	(0.0 - 14.5)
5-year-mortality %	43	

5.3 CPA in healthy liver

The investigated liver biopsies showed a mean overall CPA of 5.13 (SD=1.51) and a perivenular CPA of 3.27 (SD=0.89; see also Figure 12).

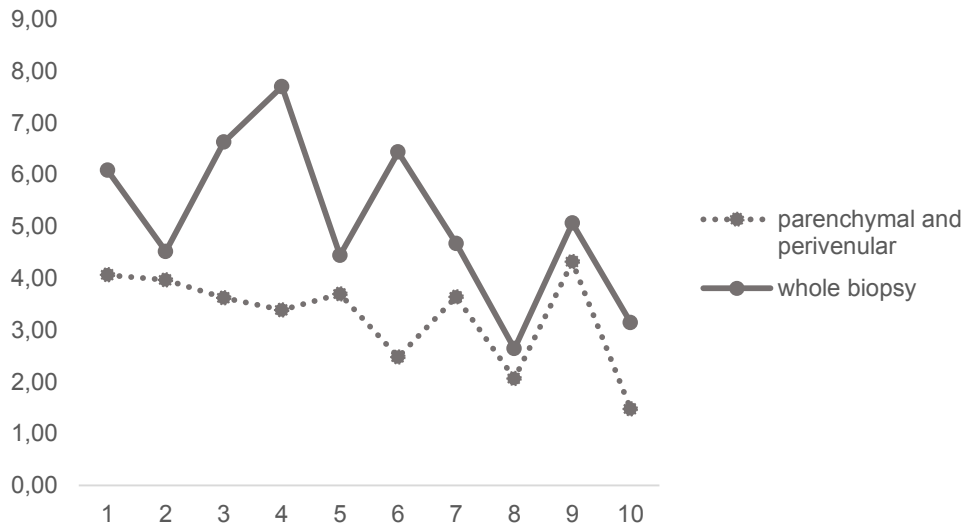

Figure 12: CPA of normal liver biopsies

5.4 Correlation of morphometric parameters with CRN stage

As Figure 13 shows, the overall CPA, septal CPA and the pericellular CPA correlate positively with the CRN stages (Figure 13ABC; overall: r=0.729, p=0.000; septal: r=0.730, p=0.000; pericellular: r=0.441, p=0.000) and whereas by contrast the PPA correlates negatively with the CRN stages (Figure 13D; r=-0.740, p=0.000).

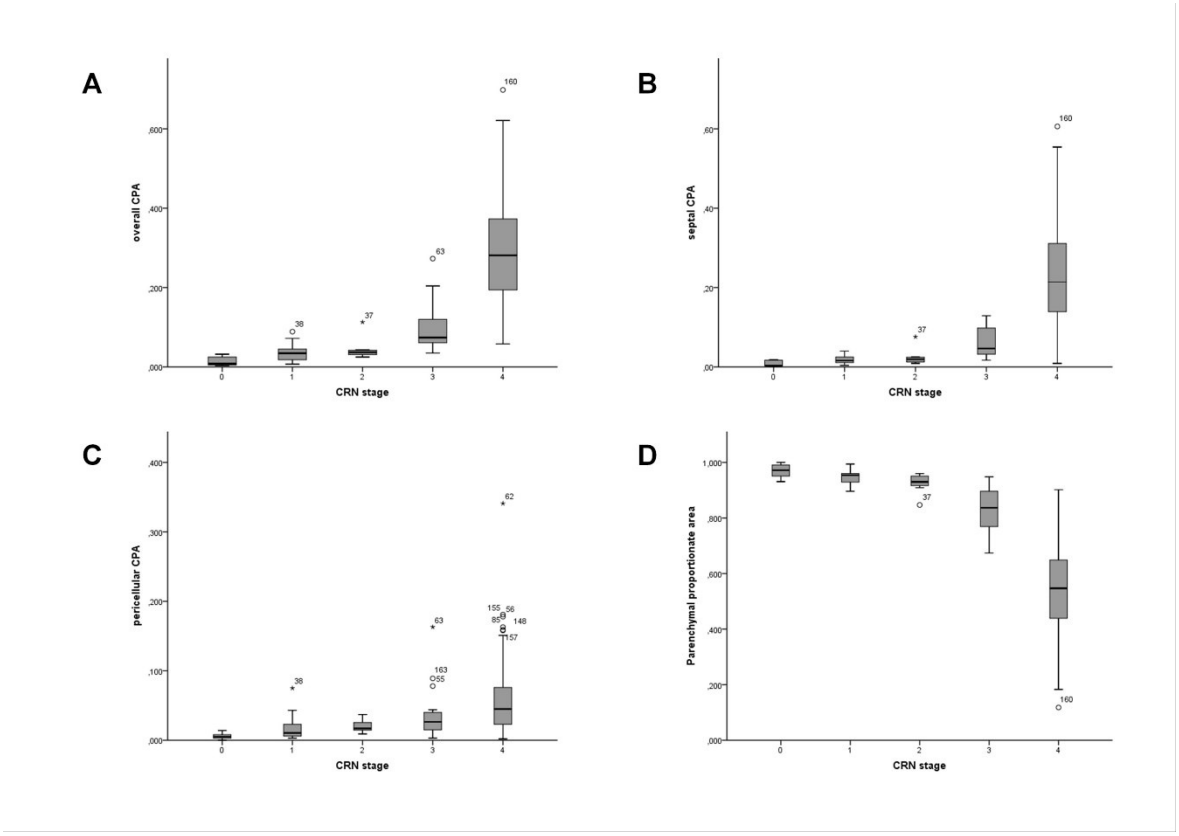

Figure 13: Correlation of morphometric features with Clinical Research Network (CRN) stage: (A, B, C) Positive correlation of overall CPA, septal CPA and pericellular CPA with CRN stages. (D) Negative correlation of parenchymal proportionate area (PPA) with CRN stages.

Morphometrically assessed steatosis in patients with CRN stage 3 and 4 decreased significantly from Stage 3 to 4 (Z=-2.707, p=0.007), correlated negatively with those stages (r=-0.710, p=0.000, Figure 14) and also correlated negatively with overall CPA (r=-0.290, p=0.001) and septal CPA (r=-0.393, p=0.000).

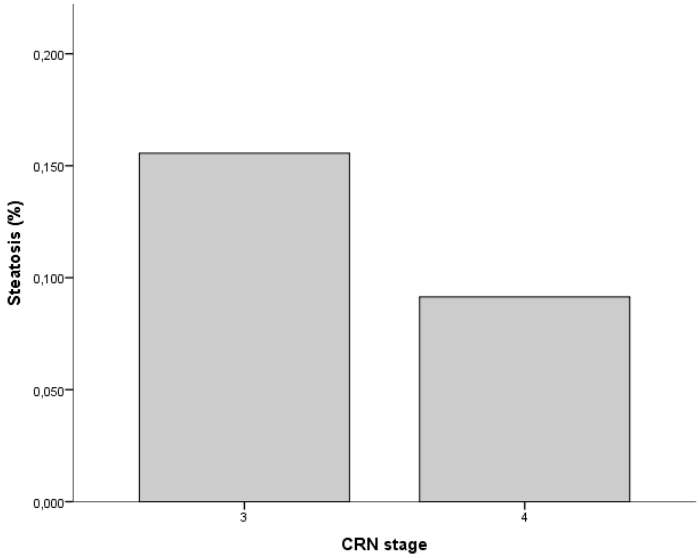

Figure 14: Correlation of steatosis with CRN stage 3 and 4.

5.5 Survival analysis

Survival analysis showed that higher overall CPA was linked to shorter 5-year-survival (p=0.046, Figure 15). Higher values in septal CPA also were linked to a shorter 5-year-survival (p=0.027, Figure 16). Pericellular CPA showed a trend toward a better outcome with higher values (p=0.090, Figure 17). Higher values in PPA as well as in pericellular CPA in proportion to septal CPA showed a longer 5-year-survival (PPA: p=0.019, Figure 18; proportion: p=0.008, Figure 19). Finally, a higher Laennec score revealed a shorter 5-year-survival (p=0.035, Figure 20). All patients were within CRN stages 3 and 4 (n=139).

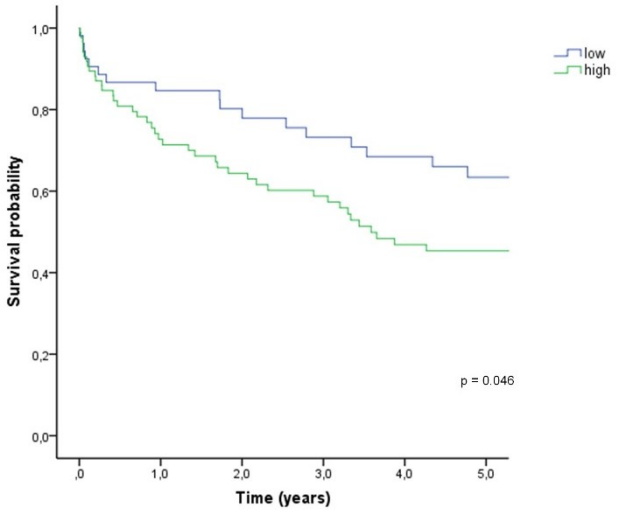

Figure 15: Kaplan-Meier plot of survival probability of patients with CRN stage 3 and 4 according to overall CPA.

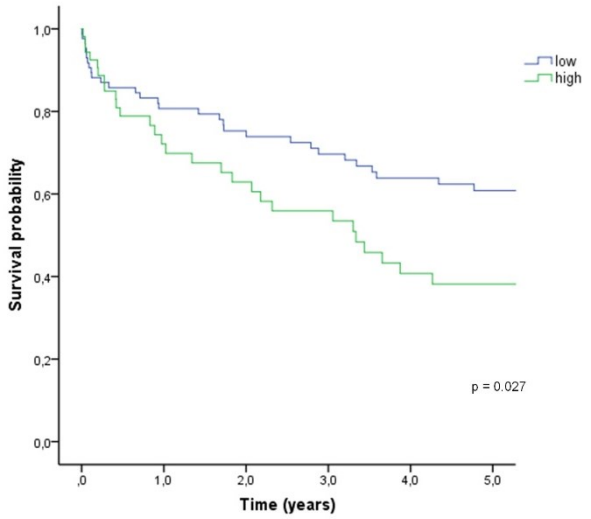

Figure 16: Kaplan-Meier plot of survival probability of patients with CRN stage 3 and 4 according to septal CPA.

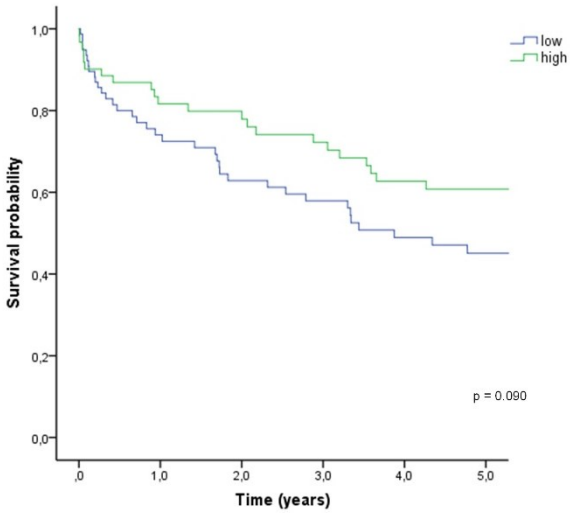

Figure 17: Kaplan-Meier plot of survival probability of patients with CRN stage 3 and 4 according to pericellular CPA.

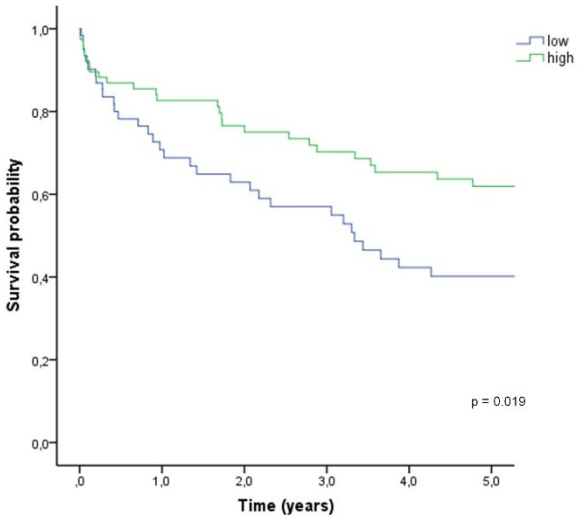

Figure 18: Kaplan-Meier plot of survival probability of patients with CRN stage 3 and 4 according to PPA.

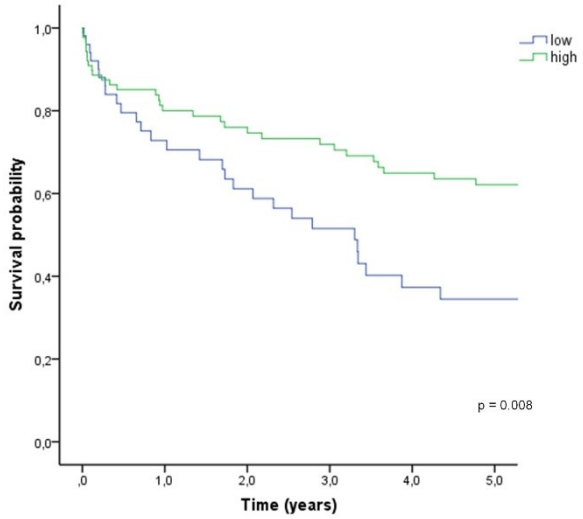

Figure 19: Kaplan-Meier plot of survival probability of patients with CRN stage 3 and 4 according to pericellular CPA in proportion to septal CPA.

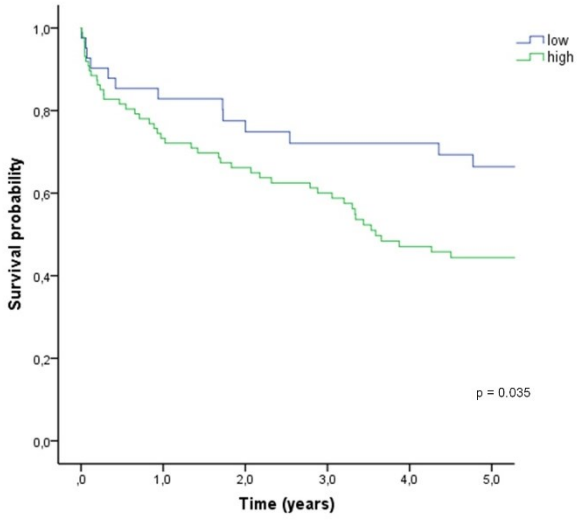

Figure 20: Kaplan-Meier plot of survival probability of patients with CRN stage 3 and 4 according to Laennec score.

Table 8: Survival analysis of patients with CRN stage 3 and 4 according to morphometric parameters (* marks statistically significant result, ** marks a statistical trend)

	AUC	cutoff	Kaplan-Maier
Overall CPA	0.569	20,75%	0.046 *
Septal CPA	0.575	23,38%	0.027 *
Pericellular CPA	0.532	4,65%	0.090 **
PPA	0.584	54,85%	0.019 *
Pericellular CPA in proportion to septal CPA	0.568	0.1592	0.008 *
Laennec score	0.617	4,5	0.035 *

In decompensated patients (n=116) higher values of pericellular CPA in proportion to septal CPA showed a longer 5-year-survival (p=0.011, Figure 21). However, there was a trend towards a shorter 5-year-survival in decompensated patients with high septal CPA and high Laennec score and a trend to a longer 5-year-survival in patients with high pericellular CPA (septal: p=0.078, Figure 22; Laennec: p=0.051, Figure 23; pericellular: p=0.076, Figure 24).

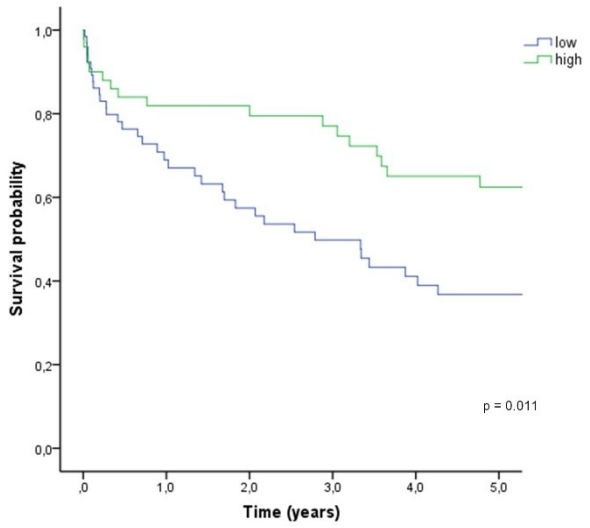

Figure 21: Kaplan-Meier plot of survival probability of patients with decompensated ALD according to pericellular CPA in proportion to septal CPA.

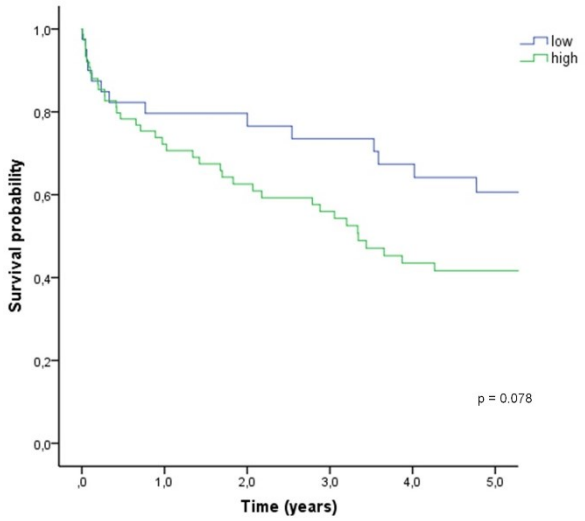

Figure 22: Kaplan-Meier plot of survival probability of patients with decompensated ALD according to septal CPA

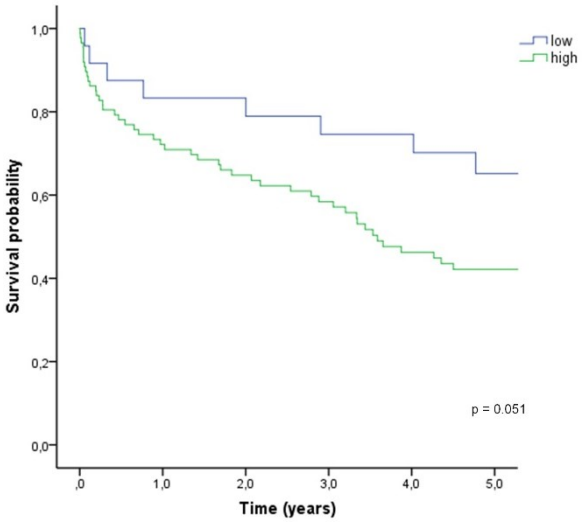

Figure 23: Kaplan-Meier plot of survival probability of patients with decompensated ALD according to Laennec score.

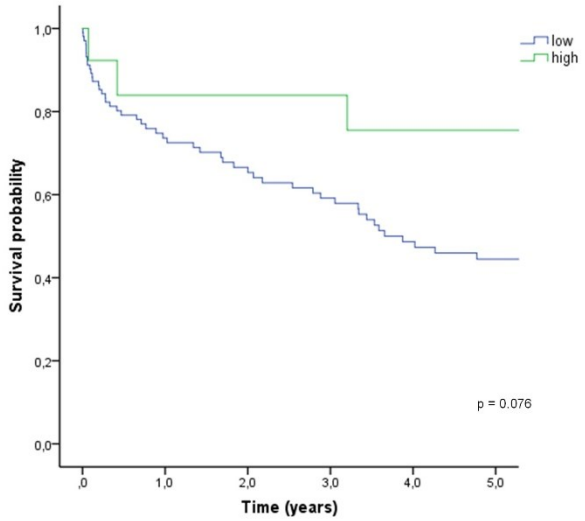

Figure 24: Kaplan-Meier plot of survival probability of patients with decompensated ALD according to pericellular CPA.

Table 9: Survival analysis of patients with decompensated ALD according to morphometric parameters (* marks statistically significant result, ** marks a statistic trend)

	AUC	cutoff	Kaplan-Maier
Overall CPA	0.526	17,75%	0.165
Septal CPA	0.541	15,75%	0.078 **
Pericellular CPA	0.549	11.85%	0.076 **
PPA	0.549	55.05%	0.135
Pericellular CPA in proportion to septal CPA	0.565	0.2831	0.011 *
Laennec score	0.564	3,5	0.051 **

In patients with compensated liver disease (n=50) higher values in overall CPA, septal CPA and Laennec score indicated a shorter 5-year-survival (overall: p=0.009, Figure 25; septal: p=0.008, Figure 26; Laennec: p=0.000, Figure 27). In contrast higher PPA values and higher pericellular CPA in proportion to septal CPA values indicated a longer 5-year-survival (PPA: p=0.017, Figure 28; Proportion: p=0.000, Figure 29).

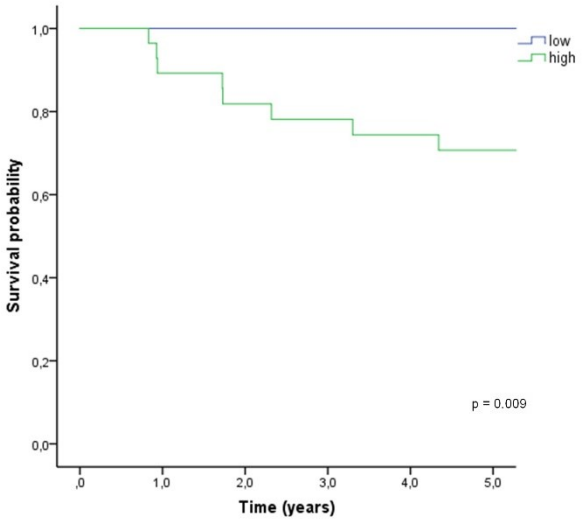

Figure 25: Kaplan-Meier plot of survival probability of patients with compensated ALD according to overall CPA.

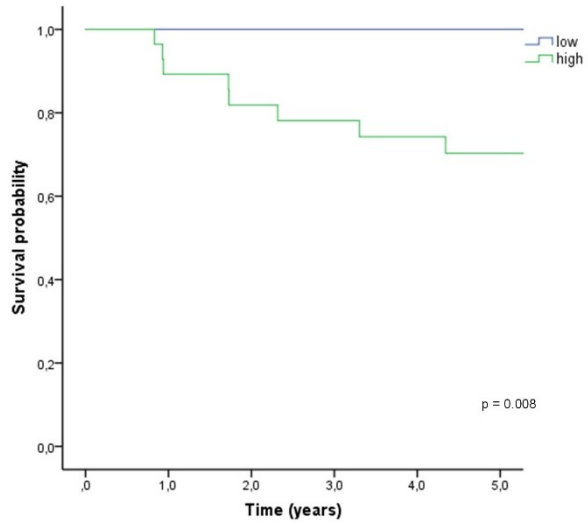

Figure 26: Kaplan-Meier plot of survival probability of patients with compensated ALD according to septal CPA.

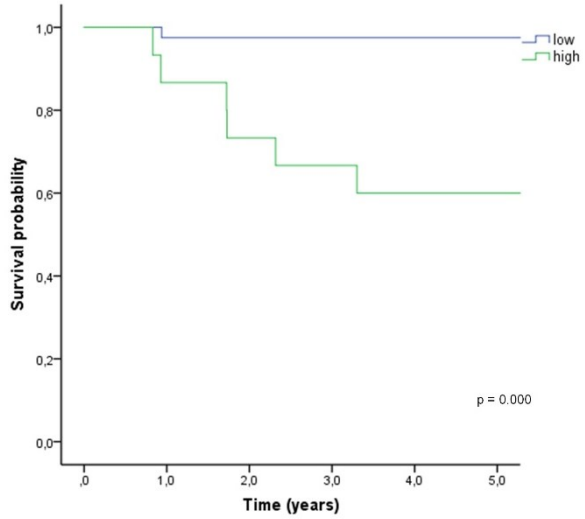

Figure 27: Kaplan-Meier plot of survival probability of patients with compensated ALD according to Laennec Score.

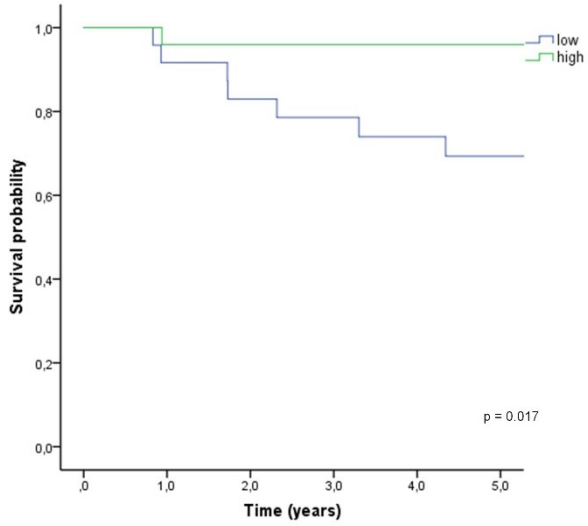

Figure 28: Kaplan-Meier plot of survival probability of patients with compensated ALD according to PPA.

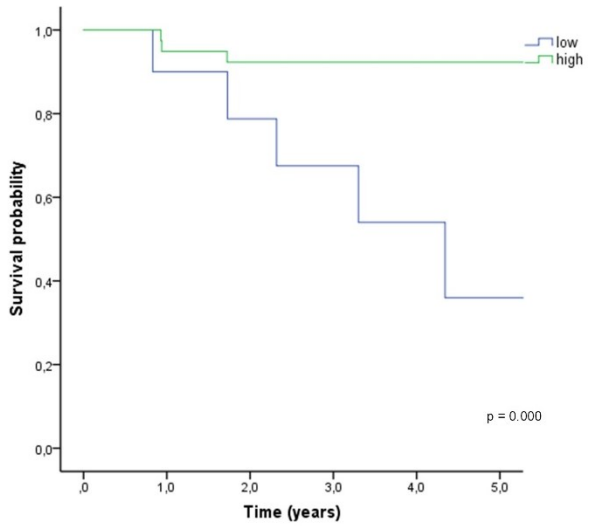

Figure 29: Kaplan-Meier plot of survival probability of patients with compensated ALD according to pericellular CPA in proportion to septal CPA.

Table 10: Survival analysis of patients with compensated ALD according to morphometric parameters (* marks statistically significant result)

	AUC	cutoff	Kaplan-Maier
Overall CPA	0.801	6.85%	0.009 *
Septal CPA	0.795	2,60%	0.008 *
Pericellular CPA	0.598	1,15%	0.104
PPA	0.783	86,00%	0.017 *
Pericellular CPA in proportion to septal CPA	0.670	0.1534	0.000 *
Laennec score	0.843	3,5	0.000 *

5.6 Correlations with biochemical parameters

Within this analysis of patients with CRN Stage 3 and 4 (n=120), various correlations were assessed with the following outcomes (Table 11):

The overall CPA showed a positive correlation with INR values (r=0.358, p=0.000) and a negative correlation with values for AST (r=-0,224, p=0.009), ALT (r=-0.363, p=0.000), GGT (r=-0.430, p=0.000) and albumin (r=-0.377, p=0.000).

Septal CPA exhibited a positive correlation with INR values (r=0.354, p=0.000) and a negative correlation with values for AST (r=-0.271, p=0.002), ALT (r=-0.328,

p=0.000), GGT (r=-0.453, p=0.000), albumin (r=-0.338, p=0.000) and platelet count (r=-0.189, p=0.028).

Pericellular CPA had a positive correlation with values for total bilirubin (r=0.196, p=0,021), leukocyte count (r=0.344, p=0.000) and platelet count (r=0.204, p=0.000).

PPA correlated positively with values for AST (r=0.236, p=0.006), ALT (r=0.355, p=0.000), GGT (r=0.442, p=0.000), and albumin (r=0.360, p=0.000) and correlated negatively with INR values (r=-0.424, p=0.000).

The pericellular CPA in proportion to septal CPA exhibited a positive correlation with values for AST (r=0.266, p=0.002), GGT (r=0.320, p=0.000), AP (r=0.222, p=0.011), leukocyte count (r=0.369, p=0.000), platelet count (r=0.303, p=0.000) and a negative correlation with INR values (r=-0.171, p=0.045).

Finally, the Laennec score correlated positively with values for total bilirubin (r=0.208, p=0.019), the INR (r=0.359, p=0.000) and negatively with GGT (r=-0.279, p=0.002), albumin (r=-0.292, p=0.001) and platelet count (r=-0.219, p=0.014).

Table 11: Correlation of biochemical parameters with morphometric features in patients with CRN stage 3 and 4. (* marks statistically significant result)

		AST	ALT	GGT	AP	Bilirubin	INR	Albumin	Leukocyte count	Platelet count
Overall CPA	r	-0.224	-0.363	-0.430	-0.101	0.103	0.358	-0.377	-0.028	-0.115
	p	0.009 *	0.000 *	0.000 *	0.256	0.230	0.000 *	0.000 *	0.744	0.183
Septal CPA	r	-0.271	-0.328	-0.453	-0.130	0.065	0.354	-0.338	-0.144	-0.189
	p	0.002 *	0.000 *	0.000 *	0.141	0.450	0.000 *	0.000 *	0.095	0.028 *
Pericellular CPA	r	0.097	-1.168	-0.023	0.123	0.196	0.095	-0.109	0.344	0.204
	p	0.265	0.053	0.791	0.163	0.021 *	0.266	0.214	0.000 *	0.017 *
PPA	r	0.236	0.355	0.442	0.135	-0.127	-0.424	0.36	0.078	0.145
	p	0.006 *	0.000 *	0.000 *	0.126	0.138	0.000 *	0.000 *	0.370	0.091
Pericellular CPA in proportion to septal CPA	r	0.266	0.095	0.320	0.222	0.096	-0.171	0.121	0.369	0.303
	p	0.002 *	0.278	0.000 *	0.011 *	0.363	0.045 *	0.168	0.000 *	0.000 *
Laennec score	r	-0.094	-0.138	-0.279	-0.052	0.208	0.359	-0.292	-0.148	-0.219
	p	0.303	0.132	0.002 *	0.575	0.019 *	0.000 *	0.001 *	0.102	0.014 *

Multiple correlations also performed in patients with decompensated ALD (n=101) had the following outcomes (Table 12):

The overall CPA showed a positive correlation with the INR (r=0.287, p=0.002) and a negative correlation with AST (r=-0.257, p=0.006), ALT (r=-0.338, p=0.000), GGT (r=-0.398, p=0.000), AP (r=-0.239, p=0.012), albumin (r=-0.320, p=0.001) and platelet count (r=-0.185, p=0.048).

The septal CPA correlated positively only with INR (r=0.274, p=0.002) and correlated negatively with AST (r=-0.286, p=0.002), ALT (r=-0.284, p=0.002), GGT (r=-0.408, p=0.000), AP (r=-0.240, p=0.012), albumin (r=-0.288, p=0.002), the leucocyte count (r=-0.202, p=0.031) and platelet count (r=-0.232, p=0.013).

Pericellular CPA had a positive correlation with leucocyte count (r=0.348, p=0.000) and a negative correlation with ALT values (r=-0.209, p=0.026).

PPA showed a positive correlation with values for AST (r=0.275, p=0.003), ALT (r=0.327, p=0.000), GGT (r=0.403, p=0.000), AP (r=0.254, p=0.008), albumin (r=0.293, p=0.002), and platelet count (r=0.208, p=0.026) and a negative correlation with INR values (r=-0.352, p=0.000).

The pericellular CPA in proportion to septal CPA showed a positive correlation with values for AST (r=0.307, p=0.001), GGT (r=0.296, p=0.001), AP (r=0.197, p=0.039), leucocyte count (r=0.419, p=0.000) and platelet count (r=0.295, p=0.001).

Finally, the Laennec score indicated a positive correlation with INR values (r=0.295, p=0.002) and a negative correlation with values for GGT (r=-0.280, p=0.003), AP (r=-0.201, p=0.040) and platelet count (r=-0.237, p=0.013).

Table 12: Correlation of biochemical parameters with morphometric features in patients with decompensated ALD. (* marks statistically significant result)

		AST	ALT	GGT	AP	Bilirubin	INR	Albumin	Leukocyte count	Platelet count
Overall CPA	r	-0.257	-0.338	-0.398	-0.239	-0.103	0.287	-0.310	-0.094	-0.185
	p	0.006 *	0.000 *	0.000 *	0.012 *	0.274	0.002 *	0.001 *	0.320	0.048 *
Septal CPA	r	-0.286	-0.284	-0.408	-0.240	-0.127	0.274	-0.288	-0.202	-0.232
	p	0.002 *	0.002 *	0.000 *	0.012 *	0.175	0.003 *	0.002 *	0.031 *	0.013 *
Pericellular CPA	r	0.073	-0.209	-0.058	-0.020	0.170	0.109	-0.051	0.348	0.120
	p	0.441	0.026 *	0.538	0.839	0.070	0.248	0.599	0.000 *	0.203
PPA	r	0.275	0.327	0.403	0.254	0.065	-0.352	0.293	0.146	0.208
	p	0.003 *	0.000 *	0.000 *	0.008 *	0.487	0.000 *	0.002 *	0.120	0.026 *
Pericellular CPA in proportion to septal CPA	r	0.307	0.098	0.296	0.197	0.219	-0.106	0.137	0.419	0.295
	p	0.001 *	0.303	0.001 *	0.039 *	0.019 *	0.260	0.157	0.000 *	0.001 *
Laennec score	r	-0.183	-0.166	-0.280	-0.201	0.024	0.295	-0.189	-0.160	-0.237
	p	0.058	0.088	0.003 *	0.040 *	0.801	0.002 *	0.052	0.097	0.013 *

Last, correlations with clinical parameters in patients with compensated ALD were attempted, with the following result (Table 13)

The overall CPA and septal CPA were positively correlated with values for total bilirubin (overall: r=0.437, p=0.002; septal: r=0.486, p=0.000), and INR (overall: r=0.619, p=0.000; septal: r=0.627, p=0.000) and negatively correlated with values for ALT (overall: r=-0.539, p=0.000; septal: r=-0.575, p=0.000), albumin (overall: r=-0.410, p=0.003; septal: r=-0.439, p=0.002) and platelet count (overall: r=-0.526, p=0.000; septal: r=-0.588, p=0.000).

The pericellular CPA correlated positively only with AP values (r=0.480, p=0.001).

The PPA exhibited a positive correlation with values for ALT (r=0.558, p=0.000), albumin (r=0.442, p=0.001), and platelet count (r=0.568, p=0.000) and negative correlations with values for total bilirubin (r=-0.461, p=0.001) and INR (r=-0.644, p=0.000).

The pericellular CPA in proportion to septal CPA showed a positive correlation with values for ALT (r=0.400, p=0.006), and platelet count (r=0.544, p=0.000) and a negative correlation with values for total bilirubin (r=-0.331, p=0.019) and INR (r=-0.450, p=0.002).

Last, the Laennec score correlated positively with values for AP (r=0.383, p=0.009), total bilirubin (r=0.457, p=0.000), and INR (r=0.566, p=0.000) and negatively with values for ALT (r=-0.412, p=0.003), albumin (r=-0.473, p=0.000) and platelet count (r=-0.517, p=0.000).

Table 13: Correlation of biochemical parameters with morphometric features in patients with compensated ALD. (* marks statistically significant result)

		AST	ALT	GGT	AP	Bilirubin	INR	Albumin	Leukocyte count	Platelet count
Overall CPA	r	-0.152	-0.539	-0.020	0.288	0.437	0.619	-0.410	-0.037	-0.526
	p	0.313	0.000 *	0.898	0.064	0.002 *	0.000 *	0.003 *	0.817	0.000 *
Septal CPA	r	-0.214	-0.575	-0.089	0.222	0.486	0.627	-0.439	-0.043	-0.588
	p	0.154	0.000 *	0.561	0.157	0.000 *	0.000 *	0.002 *	0.789	0.000 *
Pericellular CPA	r	0.041	-0.204	0.197	0.480	0.161	0.283	-0.214	0.071	-0.117
	p	0.785	0.178	0.195	0.001 *	0.264	0.054	0.140	0.656	0.446
PPA	r	0.182	0.558	0.014	-0.286	-0.461	-0.644	0.442	0.011	0.568
	p	0.225	0.000 *	0.929	0.066	0.001 *	0.000 *	0.001 *	0.945	0.000 *
Pericellular CPA in proportion to septal CPA	r	0.230	0.400	0.247	0.151	-0.331	-0.450	0.260	0.096	0.544
	p	0.124	0.006 *	0.101	0.341	0.019 *	0.002 *	0.072	0.545	0.000 *
Laennec score	r	-0.082	-0.412	0.135	0.383	0.457	0.566	-0.473	0.014	-0.517
	p	0.566	0.003 *	0.346	0.009 *	0.000 *	0.000 *	0.000 *	0.923	0.000 *

6 Discussion

The objective of our study was to evaluate in advanced ALD how pericellular fibrosis and septal fibrosis were correlated with patient outcome as well as with biochemical parameters.

Liver fibrosis is a well-known predictive parameter for liver-related mortality in all kinds of liver diseases (2). The results of our study accord with this.

It is possible to evaluate fibrosis semi-quantitatively with different scoring systems, e.g., the Laennec score (52) and the CRN scoring system (32), or quantitatively with morphometric analysis algorithms that yield more objective data. Our study showed that septal CPA is in all subgroups studied comparable to the semiquantitative Laennec score. Pericellular CPA, on the other hand, is thought to be very differently correlated with patient outcome. This is supported by favourable outcome in patients with high pericellular CPA and a high pericellular CPA in proportion to septal CPA in our study. Lackner, et. al. (6) reached similar conclusions in a semi-quantitative analysis of pericellular fibrosis. These findings indicate that pericellular fibrosis may have to be considered as offering a completely different window on patient outcome in advanced ALD.

Analysis of correlations between different CPA parameters and biochemical parameters in clinically decompensated patients supports this hypothesis. High pericellular fibrosis is associated with biochemical features completely different from those that are associated with all other measures of fibrosis, including the semi-quantitative Laennec score. Where high PCF is associated with inflammation, septal fibrosis correlates well with liver function. A possible explanation of these results is that septa contain older collagen deposits and that fibrosis of pericellular pattern represents new developed deposits. This hypothesis based on our data clearly requires further investigation.

The retrospective design of our study naturally limits our interpretations; necessary for further conclusions would be to test our hypothesis in a prospective design. Furthermore, the interpretation of our subgroup of clinically compensated patients is limited by the size of the group.

Our study clearly sets a start point for further investigations with regard to pericellular fibrosis as a distinct parameter associated with a favourable outcome

in ALD. Its conclusions may find use in development of a new scoring and staging system for ALD.

7 Attachments

7.1.1 Morphometric results (F3/F4 group)

Record #	Fibrosis (%)		Parenchyma (%)	Steatosis (%)	Thresholds	
	total biopsy	pericellular			Nucleus	Siriusred
1	3,78	1,19	94,77	17,24	0.01	0.55
2	44,46	1,05	31,60	3,86	0.01	0.55
3	51,61	15,94	24,26	7,83	0.01	0.7
4	50,01	34,10	39,23	17,78	0.01	0.65
5	21,27	4,11	64,46	13,71	0.01	0.55
6	27,27	16,32	67,44	14,51	0.01	0.7
7	44,06	4,48	45,32	11,24	0.01	0.55
8	13,33	1,99	75,38	5,22	0.01	0.6
9	30,75	4,27	55,32	5,19	0.01	0.5
10	11,73	5,08	78,09	8,70	0.01	0.6
11	7,04	4,37	91,94	27,54	0.01	0.65
12	17,06	1,12	54,98	7,42	0.01	0.5
13	3,52	1,78	92,78	16,28	0.01	0.55
14	22,02	0,93	67,91	5,02	0.01	0.55
15	34,01	3,40	43,97	2,22	0.01	0.6
16	11,06	2,43	80,43	23,06	0.01	0.6
17	21,79	10,15	57,96	9,47	0.01	0.6
18	31,85	7,94	52,02	14,61	0.01	0.55
19	21,95	4,30	60,78	2,57	0.01	0.6
20	7,56	1,78	88,40	36,77	0.01	0.7
21	29,96	11,70	50,00	7,76	0.01	0.6
22	25,60	3,26	63,52	3,66	0.01	0.6
23	6,68	0,30	81,69	9,05	0.01	0.6
24	19,74	5,41	60,69	15,45	0.01	0.55
25	4,98	0,88	73,29	21,12	0.01	0.5
26	25,38	2,00	55,97	6,01	0.01	0.55
27	33,79	14,51	52,04	8,88	0.01	0,4
28	24,22	18,08	70,68	30,92	0.01	0.65
29	11,34	0,34	68,07	2,91	0.01	0.65
30	17,37	5,59	68,34	9,57	0.01	0.55
31	10,37	0,18	74,64	8,25	0.01	0.55
32	23,45	0,74	48,44	5,23	0.01	0.7
33	26,90	15,82	64,85	4,50	0.01	0.27
34	45,86	4,77	38,65	3,80	0.01	0.7
35	34,58	6,60	42,60	29,64	0.01	0.65
36	8,93	2,82	79,39	32,47	0.01	0.6
37	24,02	1,64	51,69	16,18	0.01	0.55
38	14,29	5,78	80,94	14,31	0.01	0.6
39	37,33	16,27	49,54	19,49	0.01	0.55
40	25,24	7,07	57,06	5,46	0.01	0.65

41	29,20	5,86	49,93	12,16	0.01	0.5
42	25,68	4,19	50,71	5,32	0.01	0.65
43	69,81	9,18	11,84	8,32	0.01	0.6
44	34,29	13,15	49,58	12,64	0.01	0.55
45	30,84	4,75	44,51	5,03	0.01	0.45
46	39,62	2,91	36,58	4,24	0.01	0.55
47	31,30	4,32	54,70	4,31	0.01	0.7
48	20,40	8,92	69,00	30,54	0.01	0.5
49	37,05	9,34	52,77	5,08	0.01	0.6
50	25,38	9,53	62,96	5,38	0.01	0.65
51	13,16	3,38	79,07	5,72	0.01	0.6
52	17,84	3,88	56,05	5,74	0.01	0.45
53	20,28	12,49	70,72	16,57	0.01	0.3
54	30,45	15,11	62,74	5,73	0.01	0.85
55	15,68	1,41	64,35	4,22	0.01	0.5
56	17,75	7,71	72,40	11,47	0.01	0.6
57	7,21	0,87	86,51	6,77	0.01	0.55
58	34,21	3,12	26,85	7,92	0.01	0.4
59	13,55	4,63	72,48	4,47	0.01	0.35
60	47,29	3,42	29,18	5,87	0.01	0.6
61	37,77	7,14	43,77	8,93	0.01	0.55
62	28,05	7,40	63,29	5,53	0.01	0.65
63	39,29	7,08	43,94	6,28	0.01	0.55
64	39,62	7,59	44,33	3,12	0.01	0.55
65	32,52	3,76	39,98	4,78	0.01	0.65
66	21,47	1,40	54,63	3,39	0.01	0.55
67	19,33	1,23	65,61	7,37	0.01	0.4
68	35,73	3,90	54,10	11,22	0.01	0.6
69	6,11	2,58	90,84	11,79	0.01	0.48
70	22,89	1,88	54,73	9,57	0.01	0.37
71	56,66	6,97	20,56	12,50	0.01	0.55
72	39,25	1,89	49,12	2,10	0.01	0.55
73	33,22	9,01	49,21	9,04	0.01	0.4
74	20,81	3,79	69,77	9,21	0.01	0.5
75	7,17	3,53	86,12	4,52	0.01	0.85
76	26,98	1,69	44,41	3,54	0.01	0.55
77	19,43	1,88	57,08	4,47	0.01	0.55
78	8,88	2,84	84,79	23,91	0.01	0.5
79	52,11	5,88	33,39	5,81	0.01	0.6
80	30,40	2,42	55,81	6,53	0.01	0.55
81	10,71	7,81	82,90	9,48	0.01	0.6
82	21,77	2,75	55,52	5,28	0.01	0.4
83	27,11	17,83	64,54	17,06	0.01	0.4
84	51,11	8,03	27,61	4,00	0.01	0.4
85	27,80	9,73	50,48	9,48	0.01	0.5
86	32,55	6,34	42,66	15,03	0.01	0.55
87	50,30	0,42	31,59	2,90	0.01	0.7

88	18,23	9,16	72,43	29,21	0.01	0.45
89	38,40	4,39	31,09	15,56	0.01	0.65
90	29,59	4,99	54,61	12,59	0.01	0.75
91	17,07	10,71	73,05	24,57	0.01	0.65
92	44,12	3,90	45,50	3,05	0.01	1
93	6,15	1,03	76,94	3,92	0.01	0.37
94	48,69	11,77	39,01	6,66	0.01	0.55
95	8,19	1,70	83,25	8,62	0.01	0.5
96	50,06	11,96	30,93	17,62	0.01	0.7
97	39,63	3,84	19,11	6,31	0.01	0.4
98	33,89	2,00	34,75	2,26	0.01	0.45
99	19,90	1,95	66,06	5,25	0.01	0.55
100	19,44	5,60	71,88	22,77	0.01	0,6
101	7,90	2,25	85,89	11,74	0.01	0,6
102	19,15	5,50	62,49	5,14	0.01	0.45
103						
104	31,62	5,32	49,15	21,75	0.01	0,47
105	21,58	3,55	66,62	6,02	0.01	0,45
106	16,72	6,25	75,45	11,41	0.01	0.68
107	31,57	6,16	55,40	1,57	0.01	0.8
108	7,31	6,43	84,09	10,91	0.01	0.4
109	35,65	1,03	38,38	6,15	0.01	0.55
110	17,67	9,67	73,26	25,30	0.01	0.45
111						
112	27,67	3,22	53,93	9,21	0.01	0.6
113	23,17	1,75	56,68	15,90	0.01	0.6
114	8,93	2,32	85,19	10,00	0.01	0.75
115	20,73	4,73	64,46	3,29	0.01	0.55
116	26,61	6,68	56,60	11,42	0.01	0,7
117	14,56	1,30	74,86	3,65	0.01	0.55
118	9,49	1,22	82,65	12,99	0.01	0.65
119	39,31	0,98	42,54	4,14	0.01	0.65
120	19,37	2,43	62,09	10,89	0.01	0.7
121	41,57	1,46	40,82	1,15	0.01	0.75
122	16,76	3,91	81,20	5,45	0.01	0.55
123	44,24	14,72	49,58	9,06	0.01	0.9
124	57,61	2,15	29,08	1,46	0.01	0,8
125	49,47	4,47	34,35	3,74	0.01	0.55
126	29,45	6,05	51,45	13,78	0.01	0.68
127	36,40	5,01	46,28	6,57	0.01	0.55
128	29,63	2,12	51,11	4,29	0.01	0.6
129	62,11	11,86	18,31	8,00	0.01	0.55
130	28,62	7,94	57,71	5,01	0.01	0.38
131	20,46	10,02	64,58	2,74	0.01	0,4
132	5,84	0,88	90,18	2,45	0.01	0.55
133	38,58	3,87	39,95	7,56	0.01	0.7
134	42,26	11,22	30,21	8,18	0.01	0.55

135	5,16	1,49	84,47	19,50	0.01	0.55
136	31,85	2,81	53,52	2,89	0.01	0,6
137	7,17	4,01	89,62	11,53	0.01	0,5
138						
139	17,86	2,49	60,45	3,20	0.01	0.53
140	12,02	2,65	78,27	31,24	0.01	0,6
141	28,79	6,39	56,59	5,65	0.01	0,55
142	56,70	2,75	24,63	3,90	0.01	0.55

7.1.2 Morphometric results (F0/F1/F2 group)

Record #	Fibrosis (%)		Parenchyma (%)	Steatosis (%)	Thresholds	
	whole biopsy	pericellular			Nucleus	Siriusred
1	2,73	1,47	95,41	34,55	0.01	0,75
2	4,33	1,80	90,93	9,53	0.01	0,72
3	0,27	0,03	99,97	2,94	0.01	0,5
4	2,87	1,38	94,99	8,01	0.01	0,6
5	0,77	0,53	97,24	21,15	0.01	0,85
6	4,91	0,87	92,47	2,77	0.01	0,9
7	1,74	0,60	95,35	20,14	0.01	0,5
8	0,70	0,26	99,36	20,80	0.01	0,55
9	1,26	0,50	96,74	34,45	0.01	0,45
10	3,73	1,18	92,85	19,05	0.01	0,5
11	2,51	0,83	95,09	7,42	0.01	0,5
12	0,50	0,31	99,12	18,55	0.01	0,58
13	4,51	2,23	94,05	7,65	0.01	0,5
14	3,80	2,88	96,04	26,77	0.01	0,7
15						
16	3,37	2,05	94,85	7,63	0.01	0,5
17						
18	2,73	0,62	96,29	25,47	0.01	0,6
19	1,84	0,71	96,04	2,99	0.01	0,72
20	2,53	1,48	95,17	29,34	0.01	0,5
21						
22						
23						
24	3,17	0,47	95,57	1,90	0.01	0,5
25						
26						
27						
28	4,08	2,21	92,35	8,43	0.01	0,7
29	11,26	3,69	84,68	3,38	0.01	0,45
30	8,90	7,51	89,63	15,07	0.01	0,45
31	3,19	1,44	93,10	1,82	0.01	0,6
32						
33	3,30	0,88	92,63	2,72	0.01	0,43

34	4,14	2,31	93,01	15,73	0.01	0,6
35	7,18	4,32	90,00	22,07	0.01	0,48
36						
37	3,55	1,59	93,37	7,73	0.01	0,5

8 Literature Cited

1. World Health Organisation. Global status report on alcohol and health 2014. Luxembourg: World Health Organization; 2014.

2. EASL Clinical Practice Guidelines: Management of alcohol-related liver disease. J Hepatol 2018; 69(1):154–81.

3. Bagnardi V, Rota M, Botteri E, Tramacere I, Islami F, Fedirko V et al. Alcohol consumption and site-specific cancer risk: A comprehensive dose-response meta-analysis. Br J Cancer 2014; 112(3):580–93.

4. Corrao G, Bagnardi V, Zambon A, Torchio P. Meta-analysis of alcohol intake in relation to risk of liver cirrhosis. Alcohol Alcohol 1998; 33(4):381–92.

5. Masson S, Emmerson I, Henderson E, Fletcher EH, Burt AD, Day CP et al. Clinical but not histological factors predict long-term prognosis in patients with histologically advanced non-decompensated alcoholic liver disease. Liver Int 2013; 34(2):235–42.

6. Lackner C, Spindelboeck W, Haybaeck J, Douschan P, Rainer F, Terracciano L et al. Histological parameters and alcohol abstinence determine long-term prognosis in patients with alcoholic liver disease. J. Hepatol. 2016; 66(3):610–8.

7. Altamirano J, Miquel R, Katoonizadeh A, Abraldes JG, Duarte-Rojo A, Louvet A et al. A histologic scoring system for prognosis of patients with alcoholic hepatitis. Gastroenterol. 2014; 146(5):1231-9.e1-6.

8. Spahr L, Rubbia-Brandt L, Genevay M, Hadengue A, Giostra E. Early liver biopsy, intraparenchymal cholestasis, and prognosis in patients with alcoholic steatohepatitis. BMC Gastroenterol. 2011; 11:115.

9. Mookerjee RP, Lackner C, Stauber R, Stadlbauer V, Deheragoda M, Aigelsreiter A et al. The role of liver biopsy in the diagnosis and prognosis of patients with acute deterioration of alcoholic cirrhosis. J Hepatol 2011; 55(5):1103–11.

10. Bataller R, Gao B. Liver fibrosis in alcoholic liver disease. Semin. Liver. Dis. (Seminars in liver disease) 2015; 35(2):146–56.

11. Saunders JB, Aasland OG, Babor TF, La Fuente JR de, Grant M. Development of the Alcohol Use Disorders Identification Test (AUDIT): WHO collaborative project on early detection of persons with harmful alcohol consumption--II. Addiction 1993; 88(6):791–804.

12. Bohn MJ, Babor TF, Kranzler HR. The Alcohol Use Disorders Identification Test (AUDIT): Validation of a screening instrument for use in medical settings. J Stud Alcohol 1995; 56(4):423–32.

13. Dybek I, Bischof G, Grothues J, Reinhardt S, Meyer C, Hapke U et al. The reliability and validity of the Alcohol Use Disorders Identification Test (AUDIT) in a German general practice population sample. J Stud Alcohol 2006; 67(3):473–81.

14. Gache P, Michaud P, Landry U, Accietto C, Arfaoui S, Wenger O et al. The Alcohol Use Disorders Identification Test (AUDIT) as a screening tool for excessive drinking in primary care: Reliability and validity of a French version. Alcohol Clin Exp Res 2005; 29(11):2001–7.

15. Hildebrand M, Noteborn MGC. Exploration of the (interrater) reliability and latent factor structure of the Alcohol Use Disorders Identification Test (AUDIT) and the Drug Use Disorders Identification Test (DUDIT) in a sample of dutch probationers. Subst Use Misuse 2015; 50(10):1294–306.

16. Jeong HS, Park S, Lim SM, Ma J, Kang I, Kim J et al. Psychometric properties of the Alcohol Use Disorders Identification Test-Consumption (AUDIT-C) in public first responders. Subst Use Misuse 2017; 52(8):1069–75.

17. Hart CL, Morrison DS, Batty GD, Mitchell RJ, Davey Smith G. Effect of body mass index and alcohol consumption on liver disease: Analysis of data from two prospective cohort studies. BMJ 2010; 340:c1240.

18. Singal AK, Bataller R, Ahn J, Kamath PS, Shah VH. ACG clinical guideline: alcoholic liver disease. Am J Gastroenterol 2018; 113(2):175–94.

19. Thiele M, Detlefsen S, Sevelsted Moller L, Madsen BS, Fuglsang Hansen J, Fialla AD et al. Transient and 2-dimensional shear-wave elastography provide comparable assessment of alcoholic liver fibrosis and cirrhosis. Gastroenterology 2016; 150(1):123–33.

20. Voican CS, Louvet A, Trabut J-B, Njike-Nakseu M, Dharancy S, Sanchez A et al. Transient elastography alone and in combination with FibroTest for the diagnosis of hepatic fibrosis in alcoholic liver disease. Liver Int 2017; 37(11):1697–705.

21. Lucey MR, Mathurin P, Morgan TR. Alcoholic hepatitis. N Engl J Med 2009; 360(26):2758–69.

22. EASL clinical practical guidelines: Management of alcoholic liver disease. J Hepatol 2012; 57(2):399–420.

23. Katoonizadeh A, Laleman W, Verslype C, Wilmer A, Maleux G, Roskams T et al. Early features of acute-on-chronic alcoholic liver failure: A prospective cohort study. Gut 2010; 59(11):1561–9.

24. Maddrey WC, Boitnott JK, Bedine MS, Weber FL, JR, Mezey E, White RI, JR. Corticosteroid therapy of alcoholic hepatitis. Gastroenterology 1978; 75(2):193–9.

25. Dunn W, Jamil LH, Brown LS, Wiesner RH, Kim WR, Menon KVN et al. MELD accurately predicts mortality in patients with alcoholic hepatitis. Hepatology 2005; 41(2):353–8.

26. Pugh RN, Murray-Lyon IM, Dawson JL, Pietroni MC, Williams R. Transection of the oesophagus for bleeding oesophageal varices. Br J Surg 1973; 60(8):646–9.

27. Louvet A, Naveau S, Abdelnour M, Ramond M-J, Diaz E, Fartoux L et al. The Lille model: A new tool for therapeutic strategy in patients with severe alcoholic hepatitis treated with steroids. Hepatology 2007; 45(6):1348–54.

28. Akriviadis E, Botla R, Briggs W, Han S, Reynolds T, Shakil O. Pentoxifylline improves short-term survival in severe acute alcoholic hepatitis: A double-blind, placebo-controlled trial. Gastroenterology 2000; 119(6):1637–48.

29. Thursz MR, Richardson P, Allison M, Austin A, Bowers M, Day CP et al. Prednisolone or pentoxifylline for alcoholic hepatitis. N Engl J Med 2015; 372(17):1619–28.

30. Cabre E, Rodriguez-Iglesias P, Caballeria J, Quer JC, Sanchez-Lombrana JL, Pares A et al. Short- and long-term outcome of severe alcohol-induced hepatitis treated with steroids or enteral nutrition: A multicenter randomized trial. Hepatology 2000; 32(1):36–42.

31. Yip WW, Burt AD. Alcoholic liver disease. Semin Diagn Pathol 2006; 23(3-4):149–60.

32. Kleiner DE, Brunt EM, van Natta M, Behling C, Contos MJ, Cummings OW et al. Design and validation of a histological scoring system for nonalcoholic fatty liver disease. Hepatology 2005; 41(6):1313–21.

33. Lackner C, Tiniakos D. Fibrosis and alcohol-related liver disease. J Hepatol 2019; 70(2):294–304.

34. Lefkowitch JH. Scheuer's Liver Biopsy Interpretation. 9th ed. n.p.: Elsevier; 2016.

35. Lackner C, Gogg-Kamerer M, Zatloukal K, Stumptner C, Brunt EM, Denk H. Ballooned hepatocytes in steatohepatitis: The value of keratin immunohistochemistry for diagnosis. J Hepatol 2008; 48(5):821–8.

36. Strnad P, Zatloukal K, Stumptner C, Kulaksiz H, Denk H. Mallory-Denk-bodies: Lessons from keratin-containing hepatic inclusion bodies. Biochim Biophys Acta 2008; 1782(12):764–74.

37. Nakano M, Worner TM, Lieber CS. Perivenular fibrosis in alcoholic liver injury: Ultrastructure and histologic progression. Gastroenterology 1982; 83(4):777–85.

38. Edmondson H, Peters R, Reynolds T, KUZMA O. Sclerosing hyaline necrosis of the liver in the chronic alcoholic: a recognizable clinical syndrome. Ann Intern Med 1963; 59(5):646–73.

39. Anthony PP, Ishak KG, Nayak NC, Poulsen HE, Scheuer PJ, Sobin LH. The morphology of cirrhosis. Recommendations on definition, nomenclature, and classification by a working group sponsored by the World Health Organization. J Clin Pathol 1978; 31(5):395–414.

40. Bosman FT, Carneiro F, Hruban R.H., Theise N, editors. WHO classification of tumours of the digestive system. 4th ed. Lyon: IARC Press; 2010.

41. Mancebo A, Gonzalez-Dieguez ML, Cadahia V, Varela M, Perez R, Navascues CA et al. Annual incidence of hepatocellular carcinoma among patients with alcoholic cirrhosis and identification of risk groups. Clin Gastroenterol Hepatol 2013; 11(1):95–101.

42. Heckley GA, Jarl J, Asamoah BO, G-Gerdtham U. How the risk of liver cancer changes after alcohol cessation: A review and meta-analysis of the current literature 2011; 11:446.

43. Watanabe S, Okita K, Harada T, Kodama T, Numa Y, Takemoto T et al. Morphologic studies of the liver cell dysplasia. Cancer 1983; 51(12):2197–205.

44. Hytiroglou P. Morphological changes of early human hepatocarcinogenesis. Semin. Liver Dis. 2004; 24(1):65–75.

45. Anthony PP, Vogel CL, Barker LF. Liver cell dysplasia: A premalignant condition. J Clin Pathol 1973; 26(3):217–23.

46. Koo JS, Kim H, Park BK, Ahn SH, Han K-H, Chon CY et al. Predictive value of liver cell dysplasia for development of hepatocellular carcinoma in patients with chronic hepatitis B. J Clin Gastroenterol 2008; 42(6):738–43.

47. Le Bail B, Bernard PH, Carles J, Balabaud C, Bioulac-Sage P. Prevalence of liver cell dysplasia and association with HCC in a series of 100 cirrhotic liver explants. J Hepatol 1997; 27(5):835–42.

48. Libbrecht L, Craninx M, Nevens F, Desmet V, Roskams T. Predictive value of liver cell dysplasia for development of hepatocellular carcinoma in patients with non-cirrhotic and cirrhotic chronic viral hepatitis. Histopathology 2001; 39(1):66–73.

49. Burt AD, Ferrell LD, Hubscher S, Portmann B. MacSween's Pathology of the Liver. 6th ed. n.p.: Churchill Livingstone; 2011.

50. Zhong Z, Lemasters JJ. A unifying hypothesis linking hepatic adaptations for ethanol metabolism to the proinflammatory and profibrotic events of alcoholic liver disease. Alcohol Clin Exp Res 2018; 42(11):2072–89.

51. Higashi T, Friedman SL, Hoshida Y. Hepatic stellate cells as key target in liver fibrosis. Adv Drug Deliv Rev 2017; 121:27–42.

52. Kutami R, Girgrah N, Wanless IR, Sniderman K, Wong FS, Sherman M et al. The Laennec grading system for assessment of hepatic fibrosis: Validation by correlation with wedged hepatic vein pressure and clinical features. Hepatology 2000; 32(4):407A.

53. Calvaruso V, Burroughs AK, Standish R, Manousou P, Grillo F, Leandro G et al. Computer-assisted image analysis of liver collagen: Relationship to Ishak scoring and hepatic venous pressure gradient. Hepatology 2009; 49(4):1236–44.